TECHNISCHE UNIVERSITÄT MÜNCHEN

Fakultät für Medizin

Abteilung für diagnostische und interventionelle Neuroradiologie

Evoked response variability across alpha oscillatory sources to visual flicker stimulation: An investigation in humans using electrophysiological and blood-oxygenation recordings

Rachel Corinne Nuttall

Vollständiger Abdruck der von der Fakultät für Medizin der Technischen Universität München zur Erlangung des akademischen Grades eines

Doctor of Philosophy (Ph.D.)

genehmigten Dissertation.

Vorsitzender: Prof. Dr. Stefan Lichtenthaler
Betreuer: Priv.-Doz. Dr. Christian Sorg

Prüfer der Dissertation:
1: Priv.-Doz. Dr. Afra Wohlschläger
2: Prof. Dr. Markus Ploner

Die Dissertation wurde am 10.12.2020 bei der Fakultät für Medizin der Technischen Universität München eingereicht und durch die Fakultät für Medizin am 26.01.2021 angenommen.

Table of contents

Abbreviations

SSVEPs	Steady-state visually evoked potentials
EEG	Electroencephalography
IAF	Individual alpha frequency
BOLD	Blood-oxygenation level dependent
fMRI	Functional magnetic resonance imaging
tICA	Temporal independent components analysis
Flicker-IAF distance	The flicker frequency as an absolute distance from the IAF
Amplitude-distance correlation coefficient	The correlation coefficient describing the relationship between the SSVEP amplitude and the flicker-IAF distance
R-AR evoked amplitude	Rhythmic flicker evoked amplitude minus arrhythmic flicker evoked amplitude
R-AR BOLD beta coefficient	Rhythmic flicker BOLD beta coefficient minus arrhythmic flicker BOLD beta coefficient

Abstract

Flickering light stimulation produces steady-state visually evoked potentials (‘SSVEPs’), measurable via electroencephalography (‘EEG’) recordings, but the underpinning mechanism of SSVEPs remains disputed. The entrainment model suggests a phase-alignment of intrinsic oscillators to the flicker, whereas the superposition model postulates that the flicker-evoked response is overlaid on top of the independent intrinsic oscillatory activity. Intrinsic alpha variability has been reported across distinct spatial sources, which poses the question of multiple SSVEP generating mechanisms at the source level. This question was approached in three experiments: Experiments 1 and 2 dissociated occipitoparietal intrinsic alpha sources based on evoked responses to 1) rhythmic flicker in the alpha frequency range (6-12Hz) as a function of distance from the individual alpha frequency (‘IAF’: the peak frequency in the alpha range during eyes closed rest) and 2) rhythmic versus arrhythmic IAF flicker (with a jittered cycle length of +/-25%). In both experiments, permutation tests revealed significant variability in evoked responses across sources, supporting the idea of multiple SSVEP mechanisms at the source level. In Experiment 3, functional MRI recordings of blood-oxygenation level dependent (‘BOLD’) signal change from rhythmic IAF to arrhythmic IAF was utilised to infer specific underpinning mechanisms of the evoked responses at sources identified in Experiment 2, as a measure sensitive to intrinsic alpha amplitude changes. A linear mixed model showed no predictive relationship of the BOLD signal change on the evoked responses. Our findings support the idea of multiple SSVEP mechanisms. A simultaneous EEG-fMRI design would be well-suited for future studies aimed at investigating the exact mechanisms underlying the reported SSVEP variability across sources.

PART A

Investigating the variability in evoked responses across intrinsic alpha sources

Experiments 1 & 2

1. Introduction

Rhythmic fluctuations in neural activity are thought to form the basis of communication in the human brain (Fries et al. 2005; Gray et al., 2015), but our understanding of the exact mechanisms and functions of various oscillations remains incomplete. The 1920s marked a momentous development in the methodological opportunities for studying these oscillations: In 1924, Hans Berger invented a tool that could non-invasively measure electrical brain activity in humans: the electroencephalogram ('EEG', Berger, 1929; Millet, 2002). This tool remains a hallmark measure of human brain activity for its non-invasiveness and high temporal resolution on the scale of milliseconds.

1.1. The neural underpinnings of EEG

EEG measures the summation of extracellular field potentials generated by ion fluxes caused by synchronous postsynaptic potentials from many thousands of similarly oriented neurons. These field potentials are thought to predominantly originate from the pyramidal neurons in deep cortical layers IV and V, due to the perpendicular orientation of their apical dendrites to the cortical surface (Niedermayer & Schomer, 2012; Kirchstein & Köhling, 2009). Fluctuations across time in these field potentials, caused by a rhythmic balance between excitatory and inhibitory activity, underlie oscillatory activity (Steriade et al., 1990; Buzsaki, 2006). Oscillations have been proposed to be the building blocks of communication, supporting information transfer via phase-coupling (Bressler, 1995; Varela et al., 2001; Singer & Gray 1995; Engel et al. 2001; Fries 2005, 2009; Wang 2010).

1.2. Alpha oscillations: Origins and function

With this tool, Hans Berger discovered the so-called ‘alpha’ rhythm, the band of brainwaves oscillating at a frequency of around 8-12Hz and is the highest powered oscillatory band in humans during a state of resting wakefulness with eyes closed (Berger, 1929; Lopes da Silva et al., 1973; Niedermeyer & Lopes da Silva, 1999). Inevitably, this has led to a lot of research interest in discovering not only the origin of alpha oscillations but also the functional role that this oscillatory band plays in human cognition. Alpha oscillations have been shown to be generated by both thalamic and cortical regions, specifically the pulvinar and lateral geniculate nucleus on the one hand (Saalmann et al. 2012; Lorincz et al. 2009; Hughes & Crunelli, 2015) and infragranular cortical layers IV and V on the other (Lopes da Silva & Van Leeuwen, 1977; van Kerkoele et al. 2014; Silva et al. 1991; Buffalo et al. 2011; Mejias et al. 2016; Womelsdorf et al. 2014). Hence, alpha oscillations are thought to be generated by a mixture of both thalamocortical and corticocortical processes (Lopes da Silva, 1980).

These thalamocortical and intracortical loops generating oscillatory alpha activity, in contrast to the original proposed function of simply reflecting ‘cortical idling’ (Pfurtscheller et al., 1996), have been implicated in a number of top-down cognitive processes; Saalmann et al. (2012) demonstrated, in monkeys performing a visuospatial attention task, an increase in coherence in the alpha band between pulvinar and cortical local field potentials during trials of correct receptive-field attentional allocation, specifically in V4 and the temporo-occipital area. Samaha and Postle (2015) showed a critical role of the occipital alpha oscillatory period in the

temporal resolution of perception, with findings of flash discriminatory ability being related to the alpha cycle length. Busch et al. (2009) reported a covariance between the threshold of visual detection and the phase of ongoing alpha oscillatory activity, with 16% of light flash detection variability accounted for based on the alpha phase at which the flash was presented. An inhibitory role of alpha oscillatory activity in perception has been proposed in the 'gating-by-inhibition' model, which suggests attentional selection performance to be significantly related to the suppression of regions representing irrelevant information via GABAergic functional inhibition in the alpha range (Jensen & Mazaheri, 2010). A framework of 'cortical gain' has also been proposed by Peterson and Voytek (2017), hypothesising a cortical gain mechanism of alpha oscillatory activity by the modulation of background excitatory and inhibitory activity. Finally, alpha oscillatory activity has also been implicated in working memory, with a finding of increased alpha power with increased working memory load (Jensen et al., 2002).

1.3. Flicker stimulation produces SSVEPs

One of the frequently used tools to investigate such functions of alpha oscillatory activity is a visual flickering light stimulation. Flickering light presented at a certain frequency with a certain temporal regularity creates steady-state visually evoked potentials ('SSVEPs') that can be recorded using EEG, particularly from posterior occipitoparietal electrode recording sites (Regan, 1989; Hermann, 2001; Di Russo et al., 2007). Flicker in the alpha range has been used extensively as a tool not only to tag various responses to the processing of a particular stimulus, but also to probe the function of alpha oscillatory activity. However, research into the exact mechanism

underlying the generation of these SSVEPs has led to two dichotomous theories on exactly what this tool does in terms of the ongoing oscillatory activity, resulting in two largely different views on what this tool can be used to probe.

1.4. SSVEP-generating mechanisms

1.4.1. Model of entrainment. One field of research suggests that a rhythmic flickering light, when presented at a frequency close enough to the intrinsic alpha frequency of a given individual (i.e., the 'IAF': the frequency of maximal power within the alpha range during eyes closed rest, Koch et al., 2006), interacts with the intrinsic alpha oscillators (Schwab et al., 2006). Specifically, the proponents of this theory suggest that the alpha oscillators become 'entrained' to the flicker: the phase of the oscillator is shifted to match the instantaneous phase of the flicker, adjusting the frequency of the alpha oscillator to match that of the flicker (Hanslmayr et al., 2006; Tass et al., 1999; Mathewson et al., 2012; de Graaf et al., 2013; Notbohm, 2016; (Başar, 1980; Jansen et al., 2003; Makeig et al., 2002; Savers et al., 1974).

Two physical concepts have been utilised to infer such an interactive mechanism of the flicker on the endogenous oscillators. Firstly, the concept of the 'Arnolds Tongue' dictates that the ability of the flicker to entrain the ongoing alpha oscillators depends not only on the frequency of the flicker (the flicker frequency must be within a certain range close to the IAF), but also on the intensity of the flicker, with an interaction between the two parameters. This concept identifies, along an axis of flicker frequency and an axis of stimulus intensity, a certain region of entrainment: with weak flicker intensities, the flicker must be flickering at a frequency either at or very close to the IAF to achieve entrainment, whereas with stronger flicker intensities, the flicker

frequency can be a little further away from the IAF and still achieve entrainment (Pikovsky et al., 2003; Notbohm & Hermann, 2016). The theory of entrainment within the Arnolds Tongue suggests that we can use a flicker to interact with an ongoing oscillator in the human brain and hence probe the functional properties of alpha oscillatory activity, given that the flicker frequency is close enough to the intrinsic frequency of the endogenous alpha oscillators (with 'close enough' being defined by stimulus intensity). This theory holds clear and testable hypotheses, given that the entrained oscillator would theoretically be functionally identical to the endogenous oscillator (Schürmann et al., 1997; Hillyard et al., 1997; Herrmann, 2001; Thut et al., 2011; Mathewson et al., 2012; de Graaf et al., 2013; Spaak, 2014; Notbohm & Hermann, 2016; Gulbinaite, 2017; Keitel et al., 2014).

These testable hypotheses have been empirically supported, with evidence of non-linear effects around the IAF, suggesting an interaction with the endogenous alpha oscillatory system: Koch et al. (2006) reported maximal SSVEP amplitudes to flicker frequencies at or close to the IAF. The power of intrinsic alpha oscillators has also been reported to correlate with SSVEP amplitude (Brandt et al., 1991; Rahn & Başar, 1993a, b). Spaak (2014) showed that stimulus detection performance varies based on at which phase of a 10Hz flicker it is presented. Importantly, this effect was dependent on the distance of the IAF from 10Hz (Gulbinaite, 2017), suggesting a role of the intrinsic system.

The second concept utilisable to infer a mechanism of entrainment is one of flicker rhythmicity. Not just the frequency of the flicker itself is a factor, but also the temporal regularity of that flicker. Under this theory, a rhythmic flicker presented at/very close to

the IAF can achieve entrainment, but an IAF flicker presented at a certain arrhythmicity in terms of cycle length, does not achieve entrainment. This was shown via EEG by Notbohm and Herrmann (2016), who investigated the differences in phase-locking and target detection performance for rhythmic and arrhythmic flicker around the IAF. For rhythmic flicker, an Arnold's tongue shaped region of entrainment was found based on decreasing phase-locking values between intrinsic alpha and the flicker as a function of distance from IAF. They also reported a significant phase effect of rhythmic light stimulation on target detection performance. Such Arnold's tongue phase-locking effects and behavioural phase-dependent effects were not shown for arrhythmic flicker, controlled for intensity and average number of flickers. These results suggest a mechanism of entrainment for rhythmic, but not arrhythmic, flicker close to the IAF.

1.4.2. Model of superposition. Albeit a model with strong research support, not all research findings support the theory of entrainment; an alternative theory of 'superposition' has been proposed, which postulates independence of the ongoing oscillators from flicker stimulation (Mäkinen et al., 2004; Capilla et al., 2011). Proponents of this theory suggest that there is no interaction between the ongoing oscillators and the flicker; rather, SSVEPs are simply event-related potential responses that appear oscillatory due to the rhythmic nature of flicker presentation. Hence, this tool, in the view of this model, cannot be used to study the function of the oscillator. Rather, flicker can be used in a 'frequency-tagging' approach (Regan & Heron, 1969; Norcia et al., 2015), i.e., stimuli can be superimposed and presented at various different frequencies to enable the precise measurement of evoked responses to that particular stimuli set.

Researchers in support of this theory of superposition are those that have shown functional dissociations between the endogenous oscillators and the evoked responses. Keitel et al. (2019) showed functional disparities between the ongoing oscillator and the SSVEPs, showing that, while previous research has shown reductions in amplitude at electrode sites contralateral to an attended stimulus (Thut et al., 2006), SSVEP amplitude, on the contrary, increases. This functional disparity could not be explained by the theory of entrainment. Furthermore, Antonov et al. (2020) reported that SSVEP amplitude is unrelated to distractor suppression, a key aforementioned role of alpha oscillatory activity. Since this theory is one of non-interaction between the flicker and ongoing oscillators, but rather one of the processing of single flicker events across time, this theory would expect no difference between rhythmic and arrhythmic flickers in terms of SSVEP amplitude responses.

It is clear that there is strong evidence for both theories, albeit ones that suggest opposing mechanisms underlying the generation of SSVEPs. Oscillations measured at the scalp-level of EEG recordings represent an averaged view of underlying oscillatory activity across multiple distinct spatial sources and to distinguish between the two models may require disentangling the averaged scalp-level activity into the multiple generative sources (Haegens, 2020).

1.5. Variability at the source level

At the source level, evidence of functional, inter-, and within-individual variability has been reported (Haegens et al. 2014; Barzegaran et al., 2017). Benwell et al. (2019) investigated the variability in intrinsic alpha oscillatory parameters such as power and peak frequency across time. At the scalp-level at occipital recording sites, alpha

oscillators showed a general increase in power and a decrease in peak frequency across time. However, at the source level via a temporal independent component analysis, variability across sources of alpha oscillatory activity was found: Some sources showed only an increase in power with time, others showed only a decrease in peak frequency, and others showed a mixture of the two. These findings show variability across sources that is hidden at the scalp level. This raises the question of whether variability exists across distinct sources of alpha oscillatory activity in terms of SSVEPs to flicker in the alpha range. Such variability could offer first insight into the potential co-existence of multiple underlying mechanisms of SSVEP generation at the source level.

1.6. Research focus: Source level variability in evoked responses to flicker

To investigate the variability of SSVEPs across sources of endogenous alpha activity, we measured the evoked responses of distinct spatial sources of alpha activity to flicker in two paradigms that utilised the two concepts of Arnold's tongue and flicker rhythmicity outlined above. The first paradigm, henceforth named 'Experiment 1', investigated the evoked responses of spatial sources to rhythmic flicker as a function of flicker distance from IAF, with stimulus intensity kept constant: the theory of entrainment would expect a non-linear evoked response amplitude to flicker at frequencies around the IAF, whereas the theory of superposition would hypothesise a similar evoked response amplitude across all flicker frequency conditions. The second paradigm, described in 'Experiment 2', investigated the evoked responses of spatial sources to rhythmic IAF flicker versus arrhythmic IAF flicker: the theory of entrainment would expect a large difference in evoked response amplitude between the two

conditions, whereas the theory of superposition would expect no difference in amplitude, given the same average number of flickers across both conditions.

1.6.1. Hypotheses. We hypothesised that there would be significant variability across distinct alpha sources in terms of SSVEP amplitude to rhythmic flicker, a) at frequencies relative to IAF (Experiment 1), and b) at the IAF relative to IAF arrhythmic flicker (Experiment 2). A model of entrainment would hypothesise firstly a non-linear effect of SSVEP amplitude, with a maximal amplitude to flicker at a frequency close to /at IAF, which would decrease as flicker frequency becomes further away from the IAF (Figure 1, 'Variation 1'), and secondly a large positive difference in SSVEP amplitude of rhythmic IAF flicker minus arrhythmic IAF flicker (Figure 2, 'Variation 1'). A model of superposition, on the other hand, would expect no change in SSVEP amplitude, regardless of flicker distance from IAF (Figure 1, 'Variation 2') or flicker rhythmicity (Figure 2, 'Variation 2'). A final possible variation would also be, a) a non-linear effect around the IAF, but with a minimal amplitude at the IAF which increases with flicker distance (Figure 1, 'Variation 3'), and b) a negative SSVEP amplitude difference for IAF rhythmic flicker minus IAF arrhythmic flicker (Figure 2, 'Variation 3'). This final variation would indicate a certain interaction with the ongoing oscillator, albeit one that could not be accounted for by the traditional entrainment model.

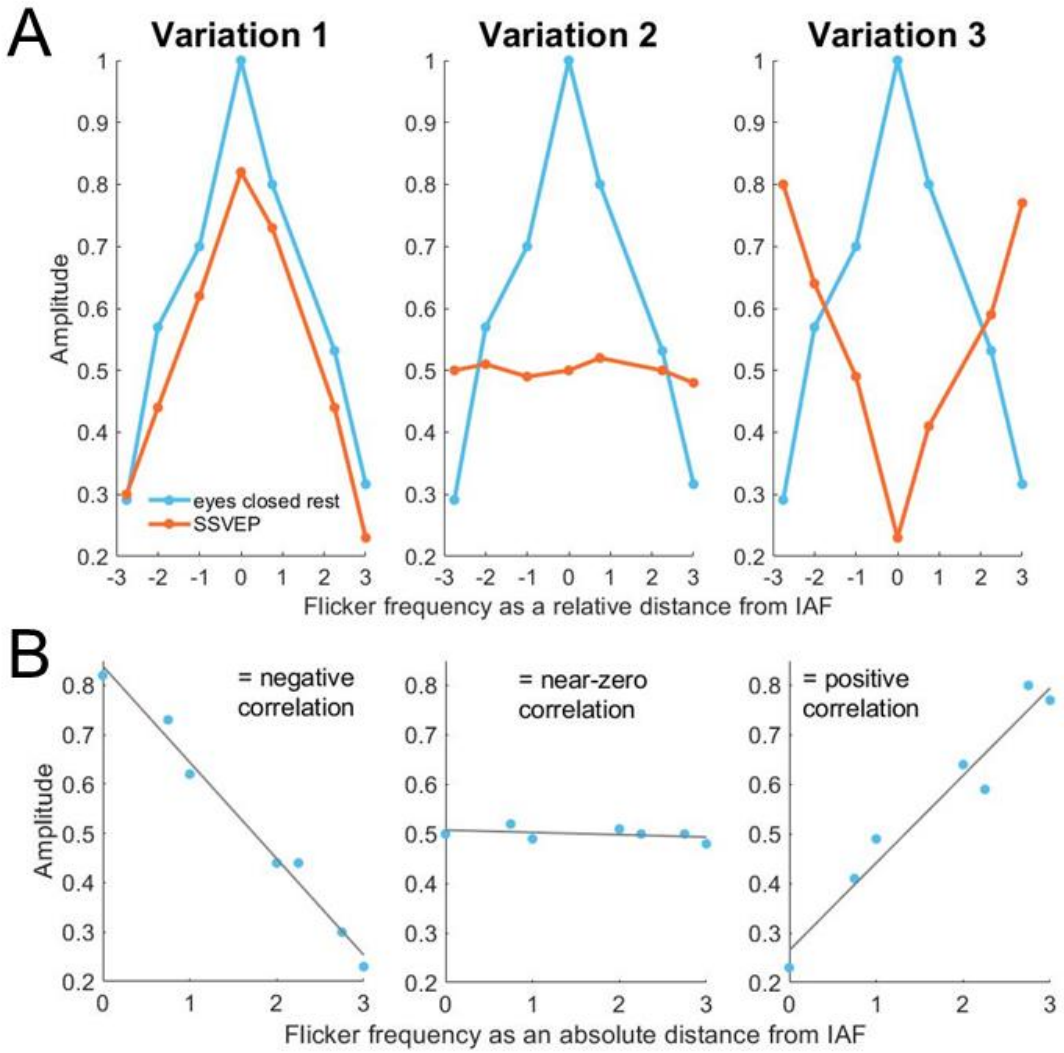

Figure 1. Hypothesised variations in SSVEP amplitude to flicker as a function of frequency distance from IAF. Panel A shows three different possible variations in SSVEP amplitude relative to the power during eyes closed rest, with the peak frequency being the IAF. Panel B shows our outcome measure for Experiment 1 of the amplitude distance correlation coefficient for each variation. Adapted from Nuttall et al., submitted.

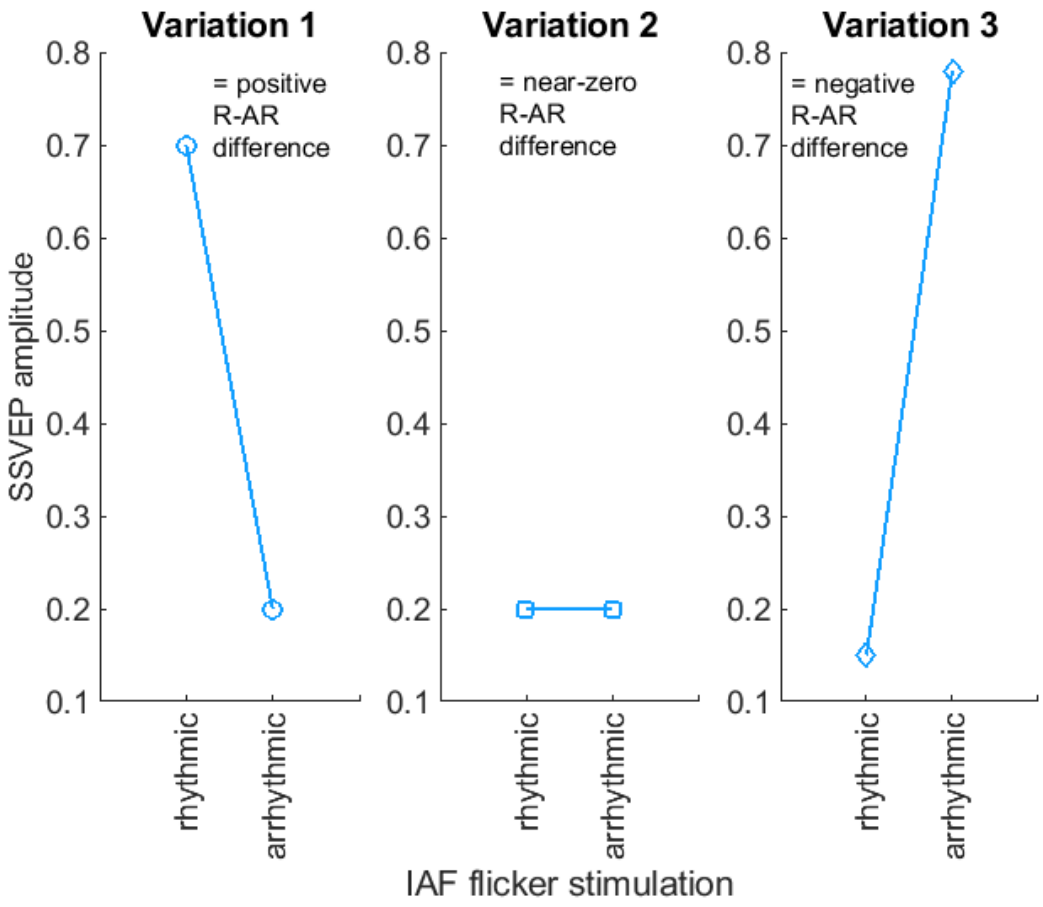

Figure 2. Hypothesised variations in the difference in SSVEP amplitude to rhythmic IAF flicker minus arrhythmic IAF flicker (R-AR difference). Three possible variations are shown.

Significant variability across sources of alpha activity in terms of a) the pattern of SSVEP amplitude as a function of flicker frequency relative to IAF, and b) the difference in SSVEP amplitude between rhythmic and arrhythmic IAF flicker conditions would indicate variability across alpha sources in terms of the way that they deal with visual flicker and would provide first insight into the possibility of multiple SSVEP generative mechanisms at the source level.

2. Materials and methods

2.1. Experimental setup

The study was approved by the local ethics committee at the Technical University of Munich and subjects provided informed consent. Subjects received financial remuneration for their participation. The experiment was carried out in a dark room with the participant lying supine on a flat surface with a height of 47cm. Placed behind the participant (150cm from their head) was a projector screen (78x98cm), behind which was a projector that displayed the visual stimuli (In Focus LP530; screen-to-projector distance of 160cm) using Presentation software (Neurobehavioral Systems, http://www.neurobs.com). The participant viewed the projector screen by looking through a mirror (at a visual angle of 71°). We chose to carry out the experiment with the participants in supine position so as to allow maximal comparability with a separate fMRI dataset taken from the same subjects. The fMRI data will be discussed in Part B.

The participant was instructed to focus on a central red fixation cross that was present throughout the experiment. The experiment consisted of alternating periods of baseline (a black screen displayed for 10 seconds) and visual flicker stimulation. Each stimulation condition consisted of 20 seconds of flicker overlaid on a low intensity radial checkerboard stimulus (luminance contrast ratio = 167L/cd/m^2). During visual stimulation, subjects were instructed to simply fixate on the cross and minimise any movement or blinking artifact. The baseline was used as a period of time for the participants to rest their eyes in between stimulation trials. The flicker was created by placing a custom-built LCD glass in front of the projector, which darkens when voltage is applied across it (further described in Dowsett et al., 2020), as controlled via a

microcontroller (Arduino Uno, Scarmagno, Italy). The flicker was hence created via a change in luminance at any chosen frequency. A 50% duty cycle was chosen so as to provide constant average luminance across all chosen flicker frequencies. The voltage pulses driving the LCD glass were logged with the EEG recording.

Experiments 1 and 2 were performed separately (on average 12 days apart) on a largely commensurate subject pool (more details given in the following sections).

2.2. Experimental design

2.2.1. Experiment 1: Evoked responses to rhythmic flicker relative to IAF

2.2.1.1. Participants. We recruited sixteen participants (mean age 26 years old, 10 female) with normal or corrected-to-normal vision with no structural brain abnormalities as identified by conventional clinical MRI assessment (FLAIR, T1, T2). Subjects reported no current use of psychoactive medication, no history of neurological disorders and no family history of photosensitive epilepsy.

2.2.1.2. Visual stimulation design. Flicker stimulation frequency conditions, preceded always by a baseline period, were presented in a randomised order, and constituted one experimental block. Chosen flicker frequencies were 6-12Hz in 1Hz steps and the 'individual alpha frequency' (IAF). Per block, each of the eight flicker stimulation frequencies were presented once rhythmically and once arhythmically, with a random jittered cycle length of up to +/- 25% of the rhythmic cycle length. Hence, each block consisted of stimulation periods with sixteen alpha flicker conditions. Experiment 1 focuses solely on the eight rhythmic flicker stimulation conditions per block. The IAF was measured from an initial 60 second eyes-closed supine rest period. The IAF,

defined as the peak frequency of intrinsic alpha activity, was identified from occipital and parietal electrodes (O1, O2, Oz, P1, P2, Pz) by segmenting the data into 4 second segments, which were baseline-corrected, Hanning-windowed and entered into a Fast Fourier Transformation (FFT). The peak frequency in the 8-12Hz range in the mean power spectrum, with a resolution of 0.25Hz for IAF specificity, was taken as the IAF for that particular participant.

The study consisted of three experimental blocks in total, with breaks in between for the participant to rest. Data from three subjects had to be excluded from analysis due to strong movement artifacts in one subject, another participant was unable to complete the testing and the other subject was initially included in the analysis pipeline but later excluded as they did not show any occipitoparietal sources of intrinsic alpha activity meeting our inclusion criteria (see section 2.4.1). Hence, we had 13 subjects' data in the final analysis, consisting of three blocks of eight rhythmic flicker stimulation periods of 20 seconds each.

2.2.2. Experiment 2: Evoked responses to rhythmic vs. arrhythmic IAF flicker

2.2.2.1. Participants. The same sixteen subjects who took part in Experiment 1 also took part in Experiment 2, alongside an additional single subject who performed only Experiment 2, totalling to 17 subjects (mean age 27 years old, 11 female) for Experiment 2, with normal or corrected-to-normal vision with no structural brain abnormalities as identified by conventional clinical MRI assessment (FLAIR, T1, T2). The additional subject also reported no current use of psychoactive medication, no history of neurological disorders and no family history of photosensitive epilepsy.

2.2.2.2. Visual stimulation design. Participants were asked to fixate on a central red fixation cross throughout the experiment and to minimise movement and blinking artifact. Identical to the IAF definition in section 2.1.2., the peak in the alpha range (8-12Hz) in the average power spectrum of 4-second segmented Hanning-windowed data from occipital and parietal electrodes (O1, O2, Oz, P1, P2, Pz) recorded from an initial 60 second eyes-closed supine rest period was taken as the IAF. There were fifteen randomised experimental conditions per block. Per condition, a low intensity radial checkerboard stimulus (luminance contrast ratio = 167L/cd/m²) was presented with a jittered flicker at the IAF overlaid for 20 seconds, preceded always by a 10 second black screen baseline period to allow the subjects to rest in between trials. The fifteen experimental conditions corresponded to fifteen different conditions of IAF flicker. The flicker was presented at the IAF but with jittered cycle lengths with the jitter extent being one of fifteen percentages of the rhythmic IAF cycle length: from 0-70% jitter extent in 5% steps. With an IAF at 10Hz for example, A 0% jittered IAF flicker corresponds to rhythmic stimulation, i.e., flicker cycle length at 100ms. A 25% jittered IAF flicker corresponds to flickers with random cycle lengths between 75-125ms. The experiment consisted of three experimental blocks with breaks in between. One subject was excluded from analysis due to the lack of a clearly discernible IAF peak in the power spectrum of the resting eyes closed data. Hence, we included 16 subjects' data in the full analysis pipeline.

2.3. Data acquisition

A 64-channel 10-20 MR-compatible EEG system (BrainAmp MR plus, Brain Products, Munich, Germany) was used with the following settings: a 250Hz online low-pass filter

(no high-pass filter was applied), a 1000Hz sampling rate, and a resolution of 0.1μV/bit (operating range ±3.28mV). An impedance of less than 10kΩ was maintained across all electrodes, with the online reference at FCz and the ground electrode at AFz.

2.4. Data analysis: Defining occipitoparietal sources of intrinsic alpha activity

All data preprocessing and analyses were conducted in MATLAB (Mathworks, v2016b), utilising the EEGLAB toolbox functions (v2019.0, Delorme & Makeig, 2004, https://sccn.ucsd.edu/eeglab/index.php) as well as Python (v3.6.4, packages 'NumPy', 'SciPy', van Rossum & Drake, 2003).

The full continuous stimulation and eyes-closed rest datasets from both Experiment 1 and Experiment 2 were initially average re-referenced and filtered using a zero-phase bandpass FIR filter (0.1-40Hz, -6 dB/octave, roll-off: [0.05Hz 40.05Hz]).

2.4.1. Experiment 1. The average re-referenced and filtered stimulation and eyes-closed rest datasets were then concatenated and entered into a temporal independent component analysis (tICA): the 60 seconds of eyes closed rest data and the 60 seconds of rhythmic flicker data for each of the eight flicker frequency conditions across all three blocks (excluding ECG electrode). The extended ICA algorithm of Lee et al. (1999), as implemented in the EEGLAB toolbox, was applied. This gave us 63 temporally independent component time series spanning the rhythmic stimulation and the resting-state eyes closed periods for Experiment 1.

We focused our analysis on occipitoparietal sources of intrinsic alpha activity. Hence, components had to meet the three criteria defined below in order to be included in the statistical analyses.

Criterium 1: Non-artifactual component. In order to automatically identify components of interest beyond artifactual components, the 63 independent components ('ICs') per participant were entered into the ICLabel toolbox (Swartz Center for Computational Neuroscience, https://sccn.ucsd.edu/wiki/ICLabel), which classifies and labels each component as most likely representing brain, muscle, eye, heart, channel or line noise, or 'other' activity based on a supervised and unsupervised Machine Learning algorithm trained on over half a million components from more than 8000 recordings. For each subject, only those components identified by the algorithm as having the highest probability of representing brain activity were used for further analysis; all other components were disregarded.

Criterium 2: Peak intrinsic frequency at IAF. The resting-state eyes closed portion of the time series of each of these 'brain' components was segmented into 4 second Hanning-windowed segments and the mean FFT across the segments was computed and entered into the FOOOF toolbox (Haller et al. 2018, https://doi.org/10.1101/299859). This toolbox allows for the identification of spectral peaks following the fitting (via an exponential function) and subsequent removal of 1/f aperiodic activity. Remaining spectral peaks are then identified in terms of their peak 'central' frequency, bandwidth, and peak power via a Gaussian fitting. For each subject, the 'brain' components with a peak frequency at the IAF (defined as a peak frequency in the range of IAF-0.25:IAF+0.25) during eyes-closed rest were taken for further analysis in order to ensure that the scalp-measure IAF, utilised as the flicker frequency of intrinsic alpha activity, adequately represents the intrinsic frequency of the components analysed.

Criterium 3: Occipitoparietal source localisation. The remaining 'brain' components with a peak intrinsic frequency at the IAF were source localised using DIPFIT (Oostenveld et al. 2011, Donders Center, University of Nijmegen). A three-shell boundary element model of the MNI standard brain was used, with singular dipoles plotted on each subject's normalised MPRAGE MRI scan (normalised via SPM12 (https://www.fil.ion.ucl.ac.uk/spm/software/spm12/), (0.75mm^3 isotropic resolution), acquired within 21 days of the EEG recording in a 3T Philips Ingenia MR scanner. The likely source origin of each component in MNI coordinates was estimated and automatically assigned a highest-probability neuroanatomical label based on the Desikan-Killiany atlas (Desikan et al. 2006). Components with a label of highest probability in occipital or parietal regions as well as a residual variance of 15% or less in terms of the overlap between the component's scalp map and the projected scalp map of the equivalent dipole were kept for further analysis. Thus, each participant had a certain number of 'chosen' components that most likely represented non-artifactual sources of occipitoparietal intrinsic alpha activity.

One subject, as mentioned in section 2.2.1.2, showed no components meeting these criteria. In total, across all remaining 13 subjects for Experiment 1, 35 occipitoparietal intrinsic alpha components were identified, with a range of 1-5 components per subject (median per subject = 2).

2.4.2. Experiment 2*.* The average re-referenced and filtered datasets consisting of an eyes-closed rest period and stimulation periods were concatenated and entered into a temporal independent component analysis (tICA): the 60 seconds of eyes closed rest data and the 60 seconds of rhythmic flicker data for each of the fifteen flicker jitter

percentages conditions across all three blocks. The extended ICA algorithm of Lee et al. (1999), as implemented in the EEGLAB toolbox, was applied. This gave us 63 temporally independent component time series spanning the jittered IAF stimulation and the resting-state eyes closed periods for Experiment 2.

Again, we focused our analysis on occipitoparietal sources of intrinsic alpha activity. Hence, components in Experiment 2 had to meet the same three criteria defined above in section 2.4.1 in order to be included in the statistical analyses. Three subjects showed no components meeting these criteria. This left us with 31 components in total across the remaining pool of 13 subjects, with a range of 1-5 components per subject (median per subject = 2).

2.5. Data analysis: Defining the evoked response of each chosen component

2.5.1. Experiment 1: SSVEP peak-to-peak amplitude. For each chosen component, the 60 seconds of rhythmic flicker per flicker frequency condition spanning all three experimental blocks were segmented into individual time-locked flicker segments and averaged, giving one SSVEP waveform per rhythmic flicker frequency condition. The peak-to-peak amplitude (maximum amplitude - minimum amplitude) of each SSVEP ('SSVEP-PtP') defined the evoked response of each component to rhythmic flicker at each flicker frequency. We used an SSVEP-PtP approach to define the evoked response in order to avoid the assumption of sinusoidal activity implicit in the FFT approach (Cole & Voytek, 2017).

At this stage, the evoked responses of our chosen components of occipitoparietal sources of intrinsic alpha activity had been characterised into one value of SSVEP-PtP

for each of the eight rhythmic flicker frequencies: 6-12Hz and the IAF. In order to characterise the evoked responses of each component in terms of the distance of the flicker frequency from the IAF, the flicker frequencies were transformed into absolute distance from IAF. For example, with an IAF of 9.25Hz, the 6Hz condition would be 3.25Hz as an absolute distance from the IAF, and the 11Hz condition would be 1.75Hz. This gave, for each chosen component, the SSVEP-PtP as an absolute distance of the flicker frequency from the IAF (termed henceforth as 'flicker-IAF distance'). A Pearson's correlation coefficient between the SSVEP-PtP and the flicker-IAF distance was measured, giving us our outcome measure of the 'amplitude-distance correlation coefficient' for each of the 35 chosen components, describing how SSVEP amplitude varies as a function of flicker frequency distance from the IAF (see Figure 1, Panel B). A negative correlation coefficient would describe a decreasing SSVEP amplitude as the flicker-IAF distance grows larger. A near-zero correlation would indicate either no change in the SSVEP amplitude with flicker-IAF distance, or SSVEP amplitudes simply following the 1/f decay. A positive correlation would describe an increasing SSVEP amplitude with an increasing flicker-IAF distance.

Control analyses*.* Our decision to use the SSVEP-PtP to define the evoked response was tested in some further control analyses. Firstly, we performed the same analysis pipeline as described, but with the use of an evoked FFT to define the evoked response to rhythmic flicker at different frequencies for each chosen component, rather than the SSVEP-PtP. For each of the 35 chosen components and each condition, the mean segment across non-overlapping 4-second segmented rhythmic flicker stimulation data was Hanning-windowed and entered into an FFT. This gave us one evoked FFT spectrum per rhythmic flicker condition per component. In each

spectrum, the absolute amplitude at the flicker frequency was transformed into signal-to-noise ratio (as defined by Cohen and Gulbinaite, 2017): The absolute amplitude at the flicker frequency was taken as a ratio to the average absolute amplitude at the surrounding frequencies (IAF+/- 2Hz, excluding +/-0.5Hz around the flicker frequency). The resulting transformed amplitude values across flicker frequency conditions were then correlated with the flicker-IAF distance via a Pearson's correlation, giving us our control outcome measure of an 'amplitude SNR-distance correlation coefficient' per component.

Secondly, we directly investigated the evoked waveform shapes per chosen component in our data by subtracting the absolute amplitude in the evoked FFT at the first harmonic of the flicker frequency from the absolute amplitude at the fundamental flicker frequency per flicker frequency condition. This analysis would result in only positive values given sinusoidal evoked responses across conditions and components. In the case of non-sinusoidal waveforms (or, alternatively, a sinusoidal response at a higher frequency), we would see negative values remaining.

These analyses provided us with two key pieces of control and confirmative information: 1) if our results based on the SSVEP-PtP definition of the evoked response are different from those utilising an evoked FFT approach, and 2) if there is evidence of non-sinusoidal evoked waveforms in our data, which would corroborate our decision of using the SSVEP-PtP approach and potentially explain any difference in results obtained via the SSVEP-PtP approach as opposed to the evoked FFT approach.

2.5.2. Experiment 2: Evoked FFT fundamental plus harmonic amplitude. For each of the 31 chosen components, the 60 seconds of data corresponding to each of the jittered IAF flicker conditions across all three blocks were segmented into 4-second segments with 50% overlap and the average segment across segments with an amplitude range below 200uV was taken. Segments with a range greater than 200uV were labelled as artifact and excluded. The average hanning-windowed segment was then entered into an FFT, giving an evoked amplitude spectrum for each jitter IAF flicker condition. The absolute amplitude at the IAF was transformed into a signal-to-noise ratio, following the same method as described above in section 2.5.1. An evoked FFT approach was taken for this experiment, as the jittered nature of the flicker made an SSVEP-PtP approach difficult to achieve without inducing bias in the peak-to-peak amplitude measure of SSVEPs based on different lengths of flicker and non-sinusoidal waveforms in our data (see below). As a result, we combined the absolute amplitude at the IAF, transformed into signal-to-noise ratio, with the transformed absolute amplitude at the first harmonic of the IAF, giving an adequate characterisation of the evoked amplitude response from variable-cycle-length flicker data with evidence of non-sinusoidal waveform shapes.

At this stage, the evoked responses of our chosen components of occipitoparietal sources of intrinsic alpha activity had been characterised into one evoked amplitude value of combined absolute amplitude at the IAF and first harmonic, for each of the fifteen jittered IAF flicker conditions. Following previous findings of loss-of-entrainment to 25% jitter and higher (Notbohm & Herrmann, 2016; Parkes et al., 2006), we focused our analysis at this stage to the difference in evoked amplitude by subtracting the 25% jittered IAF flicker condition from the 0% jittered IAF flicker condition (termed ‘R-AR

evoked amplitude'). If assuming an entrainment mechanism of evoked response generation, we would see a positive R-AR evoked amplitude difference. If assuming a superposition mechanism, we would see a near-zero difference.

This gave us our outcome measure of the R-AR evoked amplitude value for each of the 31 chosen components, describing how evoked amplitude to rhythmic IAF flicker changes as a result of arrhythmicity of the IAF flicker.

Control analyses. To find the best approach to characterise the evoked activity of sources to IAF flicker at various jitter extents, we investigated the waveform shapes of the data. For each component and per condition, the transformed (into signal-to-noise ratio) absolute amplitude at the first harmonic frequency (i.e., IAF*2) was subtracted from the transformed absolute amplitude at the fundamental frequency, i.e., IAF. As above, we would expect only positive values for purely sinusoidal waveforms, and negative values in the presence of non-sinusoidal waveforms or sinusoidal waveforms in higher harmonics dominating the signal. The presence of negative values would corroborate the inability to use SSVEP-PtP to characterise the evoked response of sources to various flicker extents. For example, a 25% jittered IAF flicker condition with an IAF at 10Hz would have cycle lengths ranging from 75-125ms. To characterise the SSVEP, one would have to artificially 'censor' all flickers to being of 75ms in length, in order to gain an SSVEP based on equal data points. Especially in the presence of non-sinusoidal waveforms, this runs the risk of artificially censoring flickers before the trough has occurred, hence giving an SSVEP-PtP value that fails to adequately characterise the amplitude of the SSVEP. The presence of negative values would also indicate that the characterisation of the evoked amplitude response to jittered flicker

from the fundamental frequency in an evoked FFT approach alone does not adequately characterise the evoked response either. In this scenario, a combined fundamental plus harmonic amplitude approach via an evoked FFT analysis would be more appropriate.

2.6. Statistical analysis

2.6.1. Experiment 1: Permutation test. We hypothesised that there would be significant variability across occipitoparietal alpha oscillators in terms of their evoked responses to flicker relative to IAF. To test this hypothesis, we measured the standard deviation across the amplitude-distance correlation coefficients and compared this value with the distribution of standard deviation values expected by chance, acquired via use of a 1000-repetition permutation test. To sample the chance distribution, on each iteration, the SSVEP-PtP values were shuffled across the rhythmic flicker frequency conditions for each component, and the standard deviation across the new set of amplitude-distance correlation coefficients was derived. The distance of our observed standard deviation from the chance distribution of standard deviation was used to calculate the resulting p-value, following the procedure described in Cohen (2017).

Control analyses. The standard deviation of the amplitude SNR-distance correlation coefficients across components was analysed for statistical significance via a permutation test with 1000 repetitions (the procedure using amplitude as signal-to-noise ratio values in exchange for the SSVEP-PtP values for performing the permutation test was the same as described directly above).

2.6.2. Experiment 2: Permutation tests. We hypothesised that there would be significant variability across occipitoparietal alpha oscillators in terms of the difference in the evoked responses to rhythmic IAF flicker (i.e., 0% jittered cycle length) versus arrhythmic IAF flicker (flicker cycle lengths jittered with a maximum jitter of 25% of the rhythmic cycle length). To test this hypothesis, a highly similar approach was taken as for Experiment 1, as outlined in the previous section. Using two permutation tests, we sampled the mean and the standard deviation of the R-AR evoked amplitude across sources that occurs as a result of chance. Per iteration, we took a new R-AR evoked amplitude value from two randomly assigned 0% and 25% jitter conditions by randomly shuffling the condition labels of jitter percentages across all true R-AR evoked amplitude values. This gave a new set of R-AR evoked amplitude values across components, from which we then took the standard deviation and the mean. Over 10000 permutations, this gave us two distributions: 1) the distribution of the mean R-AR evoked amplitude across components that occurs by chance, i.e., unrelated to specific jitter extent, and 2) the distribution of the standard deviation of R-AR evoked amplitude across components by chance. Across all permutations, the mean permuted mean value and the mean permuted standard deviation value was taken. Finally, the distance of our true standard deviation and mean values from our mean permuted standard deviation and mean values was statistically analysed using the same method as above, following Cohen (2017). This analysed the significance of not only the variance in R-AR evoked amplitude values across components, but also of the mean R-AR evoked amplitude values across components, which held relevant information for Part B, Experiment 3.

3. Results

3.1. Experiment 1: Significant variability across sources in evoked responses relative to IAF

We tested the variability across intrinsic alpha oscillatory sources in terms of their evoked responses relative to flicker distance from IAF i.e., variability of the correlation coefficients across components describing the relationship between SSVEP-PtP and flicker-IAF distance. We found a large variability across the 35 sources in terms of their amplitude-distance correlation coefficients, ranging from -0.84 to +0.93 (mean +0.2) (see Figure 3, Panel A). The observed standard deviation (0.527) was shown to be highly unlikely to occur by chance from a permutation test (p = .000056; permuted mean standard deviation = 0.3773; see Figure 3, Panel B). Hence, we found significant variability across occipitoparietal alpha sources in terms of their evoked responses to flicker relative to IAF.

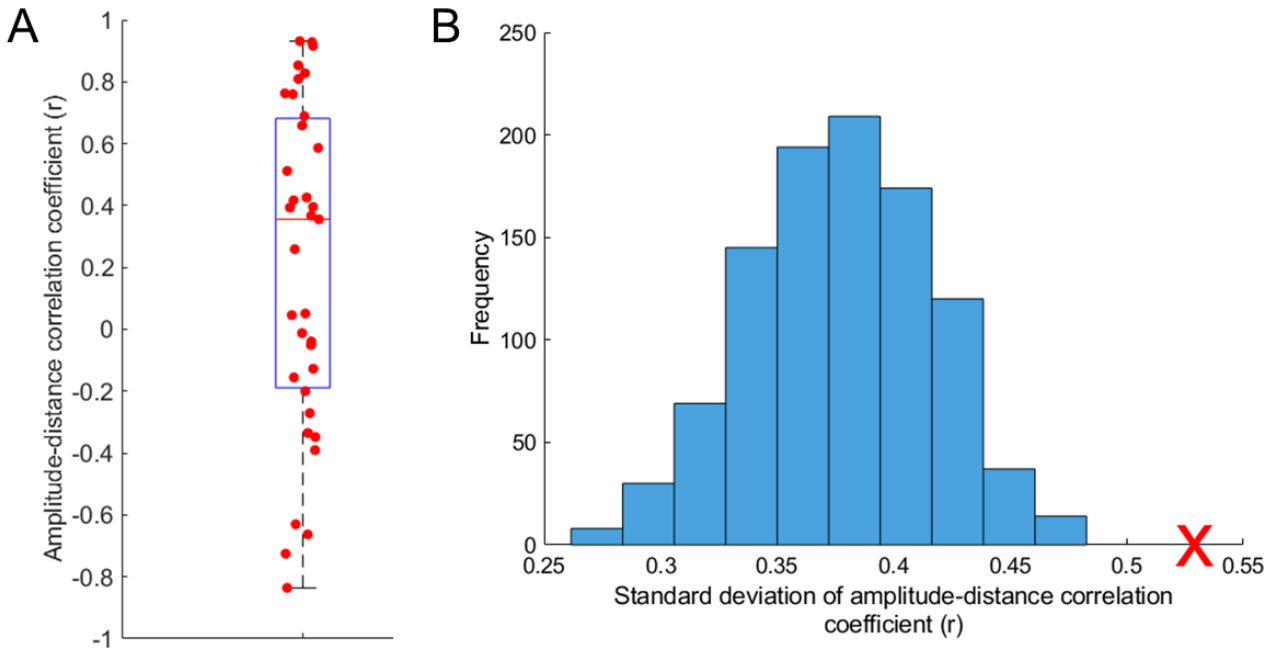

Figure 3. Panel A. Variability in the amplitude-distance correlation coefficients across occipitoparietal sources of intrinsic alpha activity. The median is shown via the horizontal red line and the top and bottom edges of the blue box representing the 75th and 25th percentiles, respectively. Panel B. The permutation test with 1000 repetitions showed that our observed standard deviation across the amplitude-distance correlation coefficients of 0.527, marked with a red cross, lies well outside of the range of standard deviation values likely to occur by chance (permuted mean standard deviation = 0.3773, shown in blue bars). Adapted from Nuttall et al., submitted.

***Control analyses*.** To control our results using the SSVEP-PtP approach of defining evoked activity, we applied the same analysis pipeline, only with the SSVEP-PtP measure exchanged for an evoked FFT signal-to-noise ratio approach. Across sources, we found a significant variability in the SNR-distance correlation coefficients (standard deviation = 0.4365, see Figure 4, Panel A). A permutation test showed this variability to be close to significance (permuted mean standard deviation = 0.3760; p = .0548, see Figure 4, Panel B).

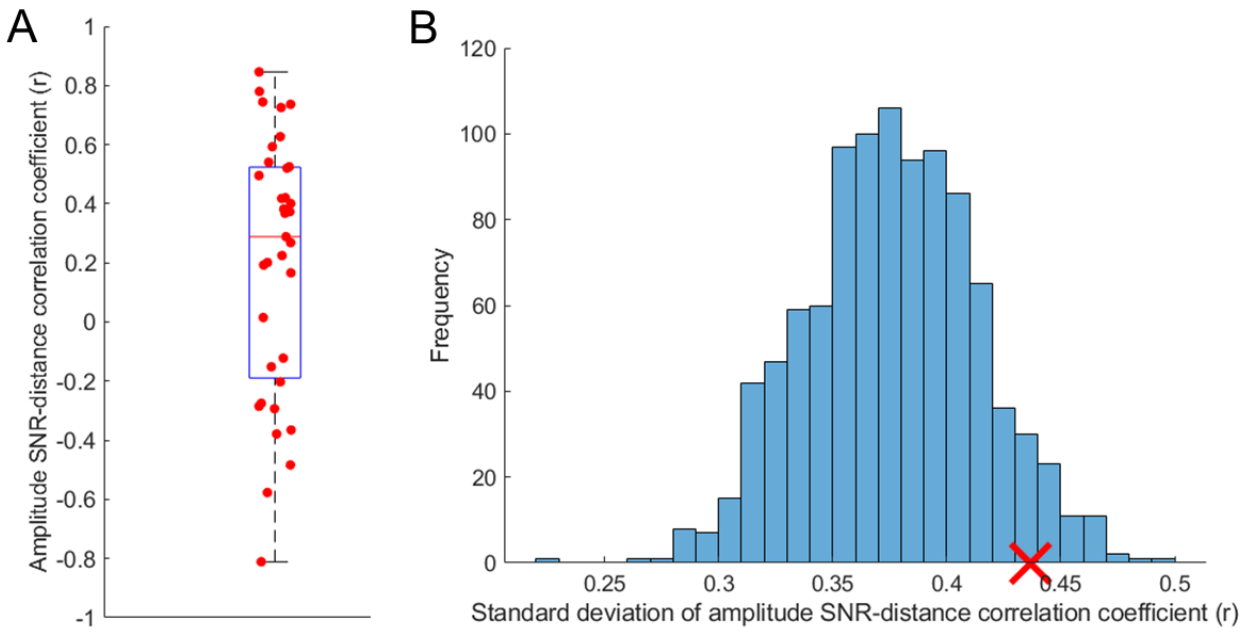

Figure 4. Panel A. Variability in the amplitude SNR-distance correlation coefficients across occipitoparietal sources of intrinsic alpha activity. The median is shown via the horizontal red line and the bottom and top edges of the blue box representing the 25th and 75th percentiles, respectively. Panel B. The permutation test with 1000 repetitions showed that our observed standard deviation across the amplitude-distance correlation coefficients of 0.4365, marked with a red cross, was approaching significance (permuted mean standard deviation = 0.3760, shown in blue bars). Adapted from Nuttall et al., submitted.

Additionally, the analysis of SSVEP waveform shapes across components and flicker conditions showed evidence of non-sinusoidal waveforms in our data (see Figure 5). When comparing the amplitude at the fundamental (i.e., flicker) frequency versus the first harmonic, we found that some sources showed lower amplitude at the harmonic than at the fundamental frequency (as would be the case for sinusoidal waveforms), and others showed higher amplitude at the harmonic than at the fundamental frequency (as would be the case for non-sinusoidal waveforms). This variability (in terms of difference in amplitude at fundamental versus harmonic frequency) existed not only across sources, but also across sources within specific subjects and across

flicker conditions within specific sources. This variability provides evidence of non-sinusoidal waveforms across various dimensions of our data, which could explain the reduced significance of our results achieved using the evoked FFT approach as opposed to the SSVEP-PtP approach: our data does not meet the assumption of sinusoidal waveforms implicit in the FFT approach. Our results validated our choice to use the SSVEP-PtP measure.

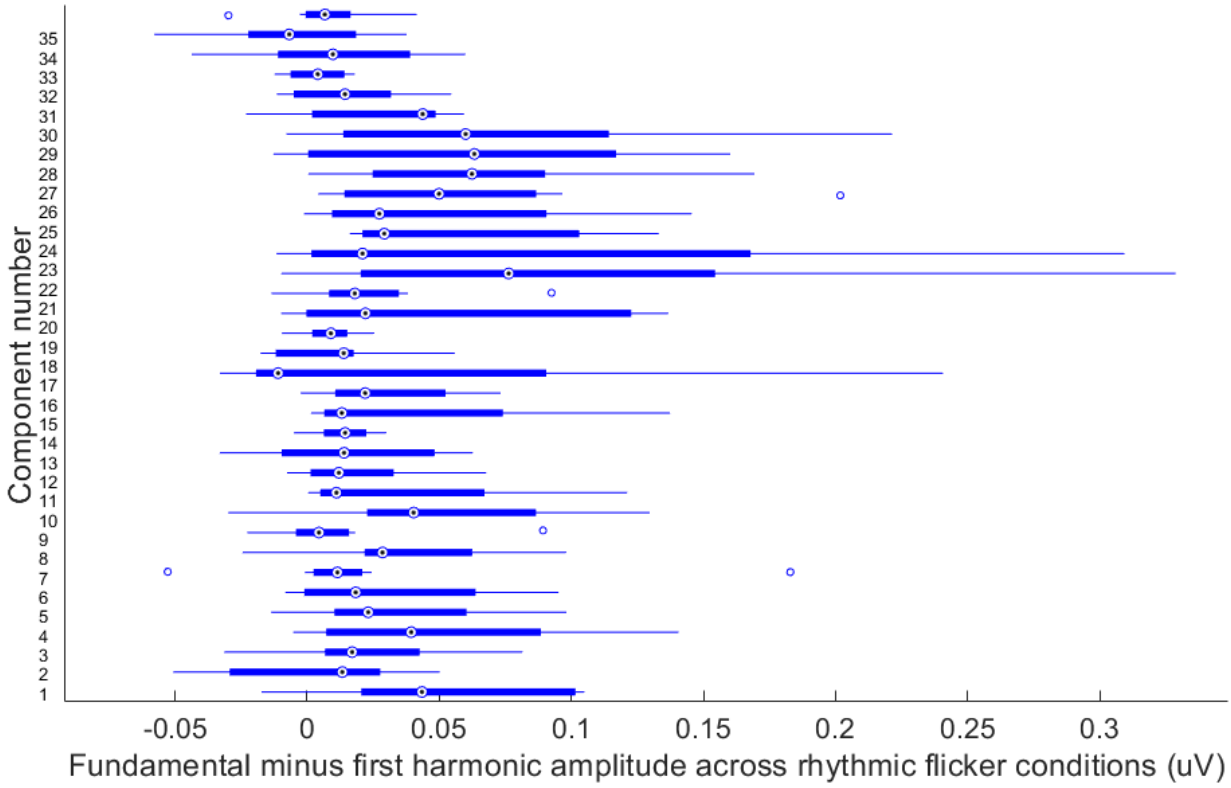

Figure 5. Investigation into the evoked waveform shapes in Experiment 1. Per component, the amplitude at the first harmonic of the flicker frequency subtracted from the amplitude at the fundamental flicker frequency across rhythmic flicker conditions is shown. The existence of negative resulting values suggests non-sinusoidal SSVEP waveforms. Adapted from Nuttall et al., submitted.

3.2. Experiment 2: Significant variability across sources in evoked responses relative to IAF flicker rhythmicity

A permutation test showed that the mean R-AR evoked amplitude value (1.924) was highly unlikely to occur by chance (p = .000005; mean across all permuted means = .001, see Figure 6). Hence, we found not only significant variability across occipitoparietal alpha sources in terms of their evoked responses to rhythmic versus arrhythmic IAF flicker, but also a significant positive mean value across all components, showing an average tendency across all components for the rhythmic 0% jitter condition to evoke higher amplitude responses than the 25% jitter condition.

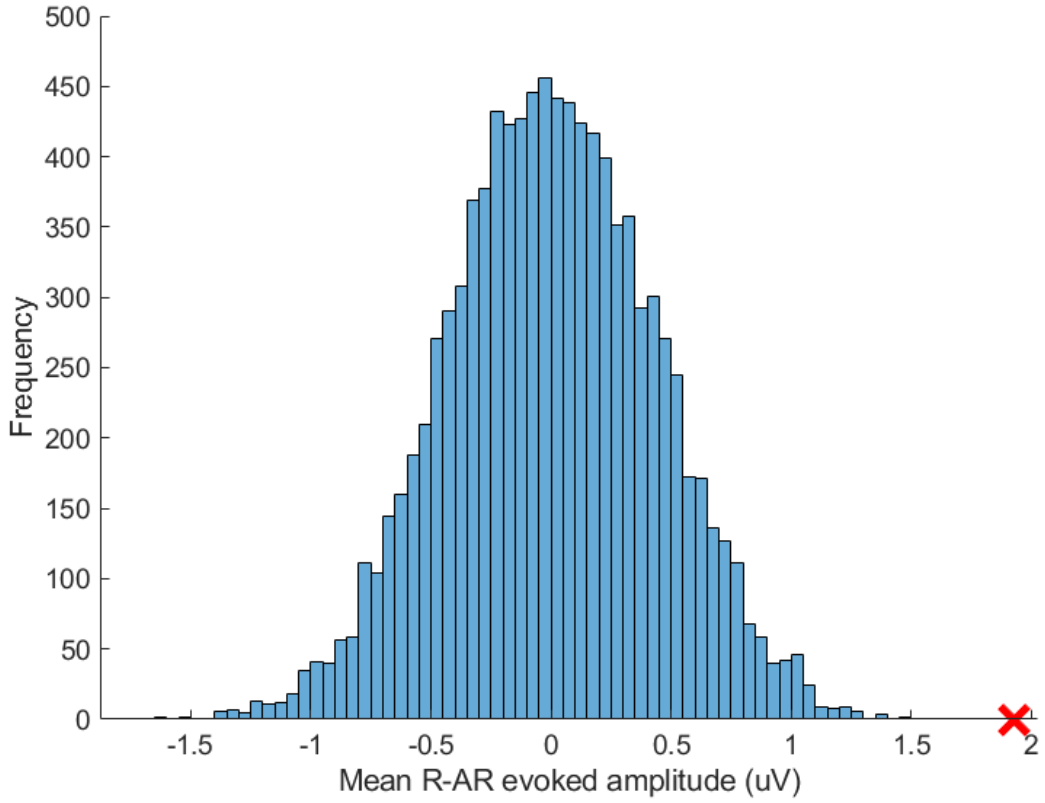

Figure 6. The permutation test with 10000 repetitions showed that our observed mean across the R-AR evoked amplitude values of 1.924, marked with a red cross, lies significantly outside

of the range of mean values likely to occur by chance (permuted mean = 0.001, shown in blue bars).

We also tested the variability across intrinsic alpha oscillatory sources in terms of the difference between their evoked responses to rhythmic (0% jitter) flicker and arrhythmic (25% jittered) flicker i.e., variability of the R-AR evoked amplitude values across components. We found a variability across the 31 sources in terms of their R-AR evoked amplitude values, ranging from -4.4633 to 12.2148 (median 1.7448, see Figure 7, Panel A). The observed standard deviation (3.4008) was shown to be unlikely to occur by chance from a permutation test (p = .025; permuted mean standard deviation = 2.3666, see Figure 7, Panel B).

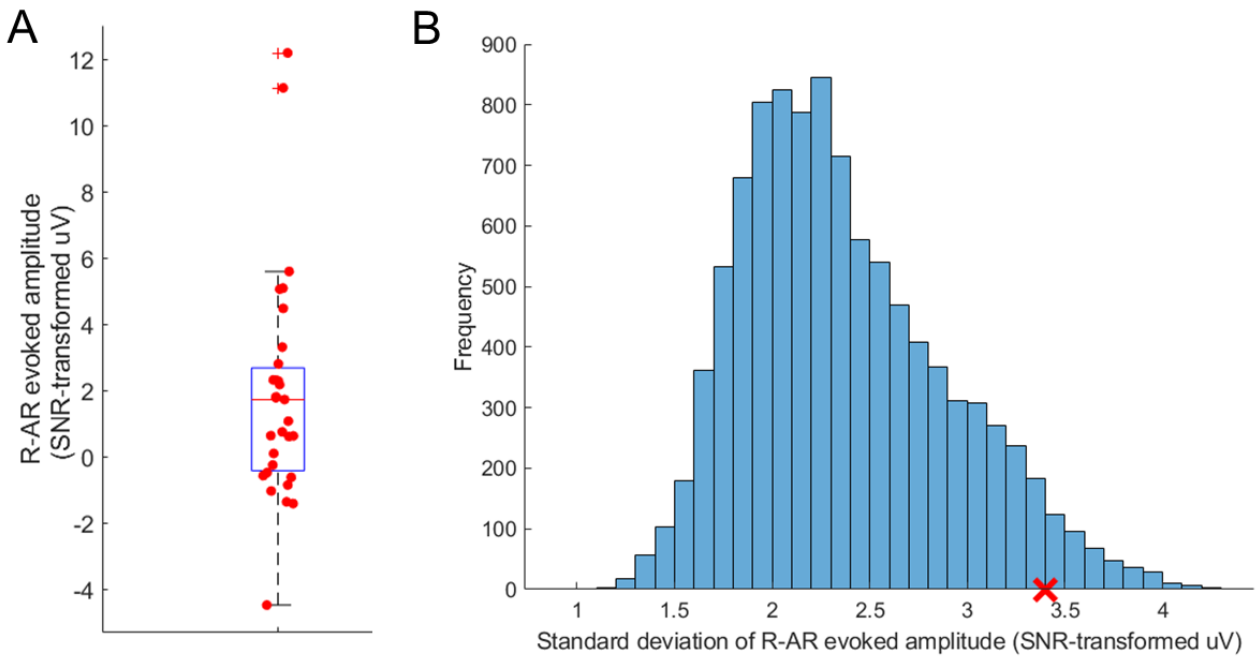

Figure 7. Panel A. Variability in the R-AR evoked amplitude values across occipitoparietal sources of intrinsic alpha activity. The median is shown via the horizontal red line and the top and bottom edges of the blue box representing the 75th and 25th percentiles, respectively. Panel B. The permutation test with 10000 repetitions showed that our observed standard

deviation across the R-AR evoked amplitude values of 3.4008, marked with a red cross, lies significantly outside of the range of standard deviation values likely to occur by chance (permuted mean standard deviation = 2.3666, shown in blue bars).

Control analyses. We investigated the waveform shapes of the evoked activity in our data by subtracting the SNR-transformed absolute amplitude at the first harmonic form the SNR-transformed absolute amplitude at the fundamental (i.e., IAF) frequency. As can be seen from the negatively and positively spanning values in Figure 8, there is evidence of non-sinusoidal waveforms in our data. This corroborated our choice of combining the SNR-transformed amplitude at the fundamental frequency with that at the first harmonic to form our evoked SNR values per condition per component: this gives us a better representation of the evoked response in data with non-sinusoidal waveforms, whilst also avoiding the problem of jittered flicker lengths that would be met with an SSVEP-PtP approach.

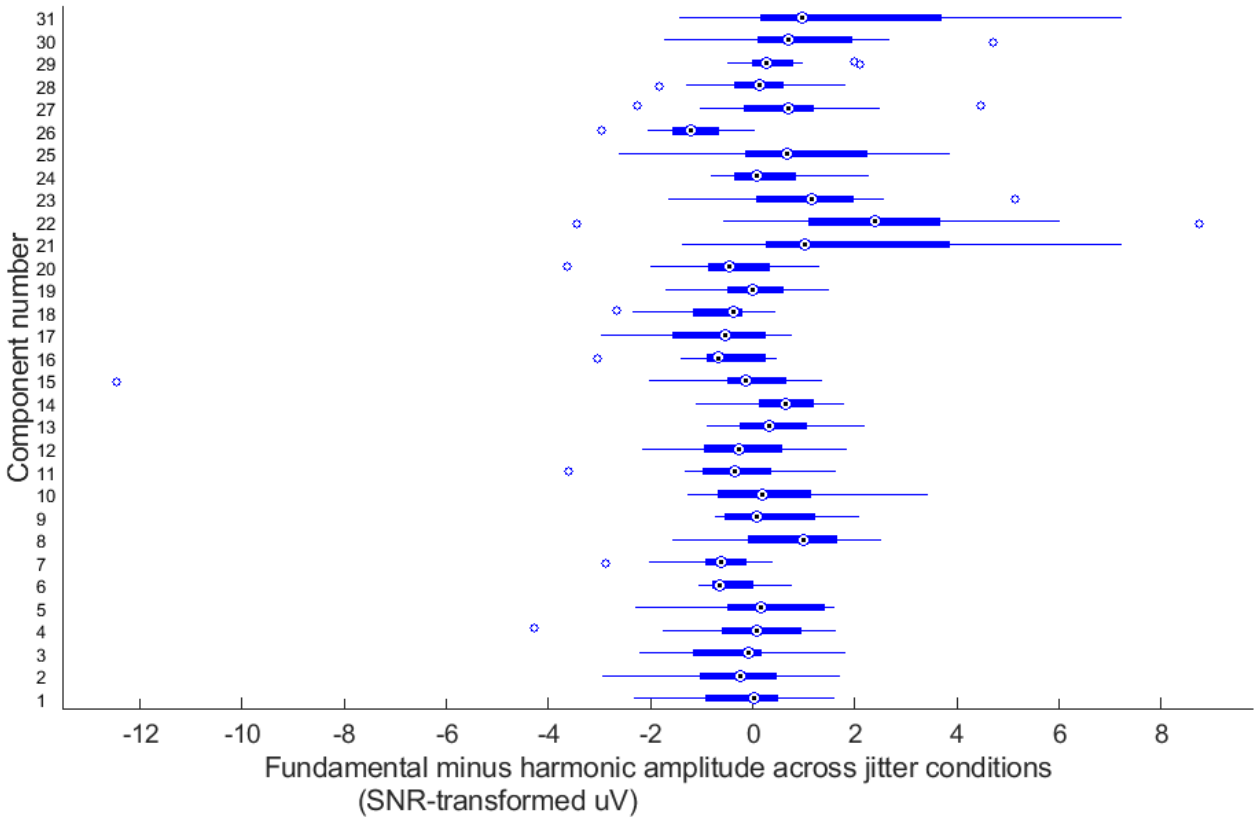

Figure 8. Investigation into the evoked waveform shapes in Experiment 2. Per component, the amplitude at the first harmonic of the flicker frequency (i.e., IAF*2) subtracted from the amplitude at the fundamental flicker frequency (the IAF) across IAF jittered flicker conditions is shown. The existence of negative resulting values suggests non-sinusoidal SSVEP waveforms.

4. Interim discussion

4.1. Different patterns of evoked responses at the source-level and possible generating mechanisms

The current study aimed to uncover the variability of SSVEPs across occipitoparietal sources of endogenous alpha activity. To investigate this variability, we measured the evoked responses of distinct spatial sources of alpha activity to flicker in two paradigms that utilised the two concepts of Arnold's tongue (Experiment 1) and flicker rhythmicity (Experiment 2) outlined above. Assuming multiple underlying mechanisms, these paradigms would lead to variability in the evoked responses measured 1) as a function of rhythmic flicker frequency distance from IAF, and 2) as a difference in amplitude between rhythmic and arrhythmic IAF flicker. In both experimental paradigms, significant variability across sources was found, suggesting the possibility of multiple underlying mechanisms in the generation of SSVEPs.

In Experiment 1, the evoked responses to rhythmic flicker as a distance from IAF, operationalised as one amplitude-distance correlation coefficient per component, showed high variability, ranging from -0.84 to +0.93. The permutation test was crucial for the statistical analysis of the variability in the amplitude-distance correlation coefficients, being based on between 5-8 data points (dependent upon where the IAF lay on the scale relative to the other flicker frequencies tested). This made the true amplitude-distance correlation coefficients prone to outliers, but the permutation test was equally sensitive to such outliers. In Experiment 2, the evoked responses to rhythmic as opposed to arrhythmic flicker at the IAF, operationalised as one R-AR evoked amplitude value per component, also showed high variability, ranging from -

4.4633 to +12.2148.

To identify where this significant variability reported in both Experiments lies in terms of intra- or intersubject variability, one must look closer at the distribution of results. Figure 9 shows the amplitude-distance correlation coefficients and R-AR evoked amplitude values split across subjects, respectively. Evidence of intersubject variability is clear from these figures, but also intrasubject variability can be seen, with approximately 50% of subjects with multiple components showing values spanning the 0 and positive and/or negative values.

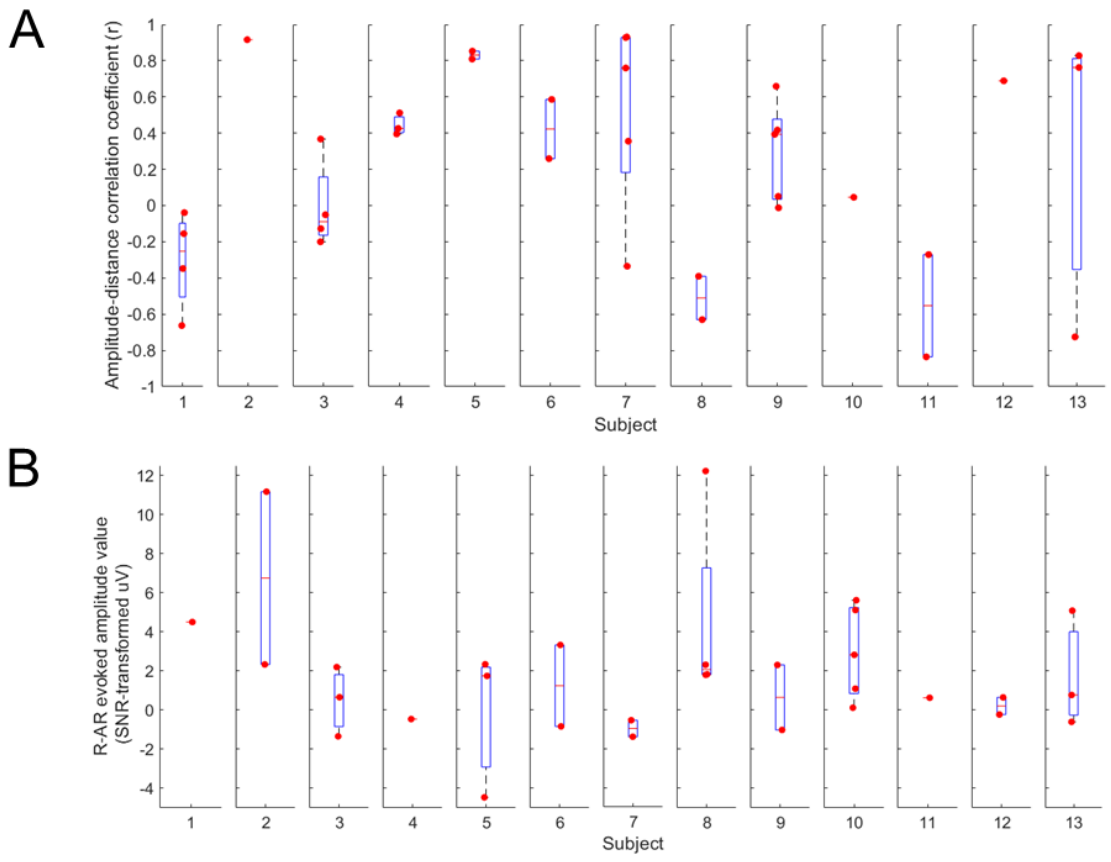

Figure 9. Intra- and intersubject variability in the amplitude-distance correlation coefficients (Panel A, Experiment 1) and R-AR evoked amplitude values (Panel B, Experiment 2). Red dots represent individual components.

Results from both experiments show variability across occipitoparietal sources of alpha oscillatory activity, with findings of positive, near-zero and negative values in both experiments. Two mechanisms, namely entrainment and superposition, have been suggested to underlie the generation of SSVEPs and, importantly, framed dichotomously; the mechanism of entrainment poses an interaction of the flicker with the ongoing oscillator (Mathewson et al., 2012; de Graaf et al., 2013; Notbohm, 2016) and hypothesises not only a nonlinear evoked response to rhythmic flicker around the IAF, but also a positive difference for the evoked amplitude during rhythmic IAF flicker minus the evoked amplitude during arrhythmic IAF flicker. The mechanism of superposition, on the other hand, poses a non-interaction and independence of the flicker from the ongoing oscillator (Capilla et al., 2011; Keitel et al., 2014; 2019), hypothesising not only no difference in the evoked amplitude to rhythmic flicker around the IAF, but also no difference in the evoked amplitude between rhythmic IAF flicker and arrhythmic IAF flicker.

Our findings of significant variability across sources in the evoked response, a) to rhythmic flicker relative to IAF, and b) between rhythmic IAF and arrhythmic IAF flicker suggests that different sources of alpha activity respond differently to rhythmic flicker at frequencies relative to IAF and relative to arrhythmic IAF flicker. These findings provide first insight into the possibility of multiple underlying mechanisms generating SSVEPs across distinct sources.

For both experiments, three ‘modes’ of evoked responses can be identified. Firstly, in Experiment 1, approximately one-third of the sources identified showed negative amplitude distance correlation coefficients, i.e., a maximal evoked amplitude to

rhythmic flicker at IAF, which decreased with increasing flicker frequency distance from IAF. In Experiment 2, approximately 50% of sources showed positive R-AR evoked amplitude values, i.e., a higher evoked amplitude response to rhythmic IAF flicker than arrhythmic IAF flicker. Both response modes would be expected under a mechanistic model of SSVEP generation where the flicker interacts with the endogenous oscillators, with their intrinsic oscillatory frequency (IAF). The model of entrainment, for example, would hypothesise such evoked responses, whereby flicker at a frequency and rhythmicity close to the IAF would entrain the endogenous oscillators and bring them into phase-alignment. As the flicker frequency and rhythmicity departs further and further away from that of the intrinsic system, the phase-alignment becomes weaker and weaker. However, our analytical focus on the evoked activity (conducted to avoid the spectral overlap problem that would be present in an induced approach) precludes any firm inferences on these evoked responses representing the mechanism of entrainment.

The second ‘mode’ of evoked responses that could be identified in both experiments was one of no change in evoked responses, regardless of experimental conditions. In Experiment 1, a near-zero amplitude distance correlation coefficient represented no change in the evoked response to rhythmic flicker regardless of flicker distance from IAF (or an evoked response pattern reflecting 1/f decay). Similarly, in Experiment 2, a near-zero R-AR evoked amplitude value represented no change in the evoked response to rhythmic IAF flicker versus arrhythmic IAF flicker. Such findings suggest a non-interaction with the endogenous alpha system, with evoked response seemingly independent from the intrinsic properties of the system, e.g., the IAF. These findings could be expected under the model of superposition, which suggests the evoked

response to flicker to be simply a summarised event-related potential response across time. Another possibility beyond oscillator independence could be one of simple non-existence of the endogenous oscillator at the given source during flicker stimulation and hence an assumption on the underlying mechanism of superposition cannot be made here.

Finally, we also found evidence in both experiments of rather unexpected, evoked response patterns. In Experiment 1, approximately one-third of sources showed a positive amplitude-distance correlation coefficient, i.e., a minimal evoked amplitude at the IAF that increased with flicker distance from IAF. In Experiment 2, this finding was not quite so apparent, with only one source showing a clearly negative R-AR evoked amplitude value. This pattern of response could not be explained by the classic mechanism of entrainment and the apparentness of this pattern in Experiment 1 led us to propose two possible mechanistic models that could result in such an evoked response.

The first model is one of ‘inhibitory-phase entrainment’, positing a specific entrainment of the inhibitory phases of the endogenous alpha oscillator to the critical i.e., light-on phases on the flicker. This would result in a minimal evoked response to flicker at the IAF, where inhibitory-phase entrainment would be strongest, and an increase in the evoked response to flicker at an increasing distance from IAF, where the inhibitory-phase entrainment would become weaker and flickers would start to ‘slip’ into the non-inhibitory phases of the endogenous oscillator. The second model is one of ‘destructive interference’ and posits the chance inhibitory-phase alignment of the rhythmic flicker to the inhibitory phases of the ongoing oscillator. The high similarity in

cycle length between the IAF flicker and the endogenous oscillator oscillating at the IAF would mean that flickers could occur in alignment with the inhibitory-phases of the endogenous oscillator just by chance, and the similarity in cycle length would mean that this inhibitory-phase alignment would then necessarily occur consistently across time, resulting in an overall minimal evoked response to IAF across the whole stimulation trial. As the flicker frequency diverges from the IAF, or becomes arrhythmic, the flicker cycle length would not match the endogenous oscillator cycle length quite so tightly, and hence the inhibitory-phase alignment would not occur as consistently across time and hence the overall evoked amplitude response across the flicker trial would increase. However, the lack of a large number of sources showing a negative R-AR evoked amplitude value, values that would be expected under the two proposed models, suggests that the positive amplitude distance correlation coefficients may not represent a robust finding.

Interestingly, the sources in Experiment 2 showed a highly significant mean R-AR evoked amplitude of 1.924, showing that, although there is a significant variability across sources, the sources show, on average, a positive R-AR evoked amplitude difference, which would be in favour of a mechanism of entrainment.

Whether the observed variability across distinct sources of intrinsic alpha activity in terms of their evoked responses to flicker of different frequencies and arrhythmicity represents the existence of multiple mechanisms underlying SSVEP generation is certainly a possibility but remains an open question. The possibility of a largely incommensurate set of SSVEP generators existing alongside our identified sources of intrinsic alpha activity remains and our focus on the evoked responses means we

cannot make any firm conclusions on the relationship between our flicker stimulus and intrinsic oscillators. Although we cannot say with certainty that SSVEPs are generated by multiple mechanisms, our findings would certainly be in accordance with such a hypothesis.

4.2. Methodological issues, limitations, and strengths

4.2.1. Sample size. The sample size in both Experiment 1 and 2 is a clear limitation (Experiment 1: N = 16 acquired; N = 13 following subject removal; Experiment 2: N = 17 acquired, N = 13 following subject removal). To some extent, our pooling of components across subjects in both experiments, our use of permutation tests to determine statistical significance and our replication of significant variability across two different experimental sessions and conditions offers some reassurance as to the robustness of our results. Notwithstanding, a replication of the study in a larger sample would be necessary to infer both intra- and intersubject evoked response variability across sources of intrinsic alpha activity.

4.2.2. Characterisation of the evoked response. The characterisation of the evoked response in each experiment was tailored to match the characteristics of the data itself, i.e., the non-sinusoidal waveforms present in both experimental datasets and the jittered waveforms in Experiment 2. In Experiment 1, an SSVEP peak-to-peak amplitude approach was taken to avoid the assumption of sinusoidal waveforms as is the case when using a traditional evoked FFT, where the power at the flicker frequency would normally be taken as the evoked amplitude response. In Experiment 2, the absolute amplitude at the fundamental frequency, transformed into SNR (relative to surrounding frequencies), was added to the absolute SNR-transformed

amplitude at the first harmonic. An evoked FFT approach was required due to the nature of the flicker data with variable cycle lengths, but the inclusion of the first harmonic frequency in the final evoked amplitude value accounted for non-sinusoidal waveforms as also shown in the dataset. The control analyses in both experiments suggest that our results are reliable and based on the appropriate measures for the characterisation of the evoked responses.

4.2.3. Experimental setup. When interpreting our results and comparing them with those from other studies, one must remember that the subjects performed both experiments in a supine position. This was done to ensure maximal comparability with a functional MRI dataset (discussed in Part B) acquired from the same subjects and on the same day as Experiment 2. The resting cortical state is significantly altered by body position (Thibault et al., 2014; Spironelli et al., 2017): changes in the alpha band in terms of amplitude is reportedly sensitive to body position, with the supine position inducing cortical inhibition (Spironelli et al., 2016). These studies, albeit focused on the resting state rather than on a task state, such as during flicker stimulation, suggest the supine position may be a factor to take into consideration.

4.3. Conclusion: Significant evoked response variability across intrinsic alpha sources suggests multiple underlying SSVEP mechanisms

We can conclude from the results of both experiments that the evoked responses to rhythmic flicker, both relative to IAF and relative to arrhythmic flicker, vary significantly across distinct occipitoparietal alpha oscillators. This finding shows that different sources of alpha oscillatory activity deal differently with visual flicker and provides first insight into the possibility of multiple underlying mechanisms in the generation of

SSVEPs. A future replication of the finding on more subjects with a design that enables the analysis of induced activity changes to flicker would provide stronger evidence for multiple SSVEP generating mechanisms. For example, the blood-oxygenation dependent (BOLD) signal in humans has been shown to be sensitive to intrinsic fluctuations in alpha amplitude. A concurrent measure of the BOLD signal during flicker stimulation could provide deeper insight into the induced changes in the intrinsic oscillators imposed by the flicker and hence the potential mechanisms underlying our evoked response patterns and the variability thereof. This is the focus of Part B: Experiment 3.

PART B

Investigating the mechanistic underpinnings of the evoked response variability across intrinsic alpha sources

Experiment 3

5. Introduction

5.1. Blood-oxygenation measure as a proxy of neural activity

A second hallmark measure utilised to infer relationships between human brain activity and cognitive function is the blood-oxygenation level dependent (BOLD) signal via functional magnetic resonance imaging (fMRI), which has been shown to be sensitive to changes in brain metabolism (Kwong et al., 1992; Ogawa et al., 1990). This measure takes advantage of the local magnetic susceptibility effects of deoxyhaemoglobin, altering the local MR signal due to magnetic field distortions within and around the blood vessels (Buxton et al. 2004). The non-linear hemodynamic response is a collective term used to refer to the set of physiological responses to neuronal activation: changes in the cerebral blood flow, cerebral blood volume, and cerebral metabolic rate of oxygen. Increased neural activity leads to a transient decrease in oxyhaemoglobin, following which the increased cerebral blood flow with the relatively slower cerebral metabolic rate of oxygen leads to a decreased oxygenation extraction fraction and hence less deoxyhaemoglobin (Fox & Raichle, 1986). This translates into an increase in the BOLD signal, given the reduced magnetic field distortions.

The relationship between neural activity and the hemodynamic response (termed ‘neurovascular coupling’), however, is not straightforward; the BOLD signal is only a proxy measure of neural activity, and the exact relationship between the BOLD signal and neural activity is not fully understood (Logothetis et al. 2008). Despite this complexity, studies have shown that the BOLD signal correlates with changes in the

local field potential, rather than local spiking activity (Lauritzen, 2001; Lauritzen and Gold, 2003; Logothetis, 2002; 2003; Logothetis et al., 2001) and suggests that the BOLD measure can be used to infer relative changes in oscillatory neural activity.

5.2. BOLD fluctuations are inversely coherent with intrinsic fluctuations in alpha amplitude

A negative relationship between fluctuations in intrinsic alpha power and the BOLD signal in the occipital, parietal, superior temporal, inferior frontal, and cingulate cortical regions has been extensively reported (Feige et al., 2005; Goldman et al., 2002; Moosmann et al., 2003; Laufs et al., 2003; Fuglo et al., 2012; Scheeringa et al., 2009; 2011; Liu et al, 2016; Koch et al. 2006). This inverse relationship has been related to both an indirect effect of decreased metabolism via reduced cortical excitability as a result of functional inhibition (Feige et al., 2005; supported by findings of reduced functional connectivity within the visual system with increased alpha power: Scheeringa et al., 2012) and a direct effect of decreased metabolism via a mean shift in membrane potential towards a less depolarised state (Hermes et al. 2017). Hence, reductions in BOLD amplitude occur with an increase in power of intrinsic alpha oscillators, thought to represent reductions in metabolism. This suggests that fluctuations in the BOLD signal can be used as a proxy for intrinsic fluctuations in alpha amplitude.

5.3. The evoked BOLD response to flicker stimulation

The BOLD signal is sensitive to both background oscillatory activity and task-evoked activity and several studies have investigated the effects of rhythmic visual flickering stimulation on the BOLD signal. They have verified the widely reported increase in the

BOLD signal up to around 6-8Hz (Kwong et al, 1992; Singh et al., 2003; Ozus et al., 2001; Parkes et al., 2004), with a generally reported plateau thereafter. Evidence of a reduction in the BOLD signal at around 10Hz flicker stimulation can be seen in some of these studies, given a visual stimulation design that would allow the identification of a within-alpha band reduction in the BOLD signal. Ozus et al. (2001) used flicker frequencies up to 20Hz and showed a reduction in the BOLD signal at 10-12Hz flicker stimulation compared with higher frequencies. This reduction was also shown by Parkes et al. (2004), who found not only an overall decreased BOLD response to rhythmic flicker in the alpha range as compared with flicker presented arrhythmically, but also a maximal reduction within the alpha range at 10Hz can be seen in their results for the rhythmic flicker conditions only. This reduced BOLD to exclusively rhythmic 10Hz flicker, with equal number of flickers as the 10Hz arrhythmic flicker condition, suggests a superposition of the evoked BOLD response on the BOLD signal fluctuations imposed by intrinsic alpha fluctuations.

5.4. The BOLD response as a linear summation of flicker-evoked response and alpha-amplitude coherent fluctuations

Fox et al. (2006) reported that a significant proportion of the variability in the event-related BOLD response can be attributed to spontaneous fluctuations in the brain activity, with the task-related activity linearly superimposed on top. Becker et al. (2011) reported a similar finding in a simultaneous EEG-fMRI study, showing that variability in the evoked BOLD response to a static visual stimulus presentation across trials could be significantly explained by intrinsic alpha power in extrastriate, thalamic and cerebellar regions. Given BOLD reductions to increased intrinsic alpha amplitude, with

the evoked response superimposed on top, the BOLD signal could potentially be utilised to infer the presence of interaction with or independence from the intrinsic oscillatory activity during conditions of visual flicker.

5.5. Research focus: The BOLD response to visual flicker at alpha oscillatory sources to infer the underlying SSVEP mechanism

In Experiments 1 and 2, we showed significant variability across sources of intrinsic alpha oscillatory activity in terms of their evoked responses to rhythmic IAF flicker relative to flicker frequencies further away from the IAF and relative to arrhythmic IAF flicker. The different patterns of evoked responses observed could be explained by the mechanistic models of entrainment, i.e., the intrinsic oscillator is shifted into phase-alignment with the flicker, and superposition, i.e., the flicker-evoked response is overlaid on the independent background oscillatory activity. However, such underlying mechanisms of evoked responses to visual flicker and the variability thereof cannot be concluded from our results, given our focus on the evoked amplitude changes only.

The BOLD signal can offer further insight into the mechanistic underpinnings of the variable evoked responses across sources of alpha oscillatory activity. Sources that showed a positive difference in the evoked amplitude between rhythmic and arrhythmic IAF flicker could be explained by the model of entrainment. In the BOLD domain, a reduced BOLD response to rhythmic IAF flicker as compared with arrhythmic IAF flicker (with the same number of flickers across conditions) at these sources would support such an underlying mechanism of interaction and possibly entrainment, as the increased evoked amplitude to rhythmic IAF flicker could be

attributed to a change in the intrinsic amplitude of the alpha oscillator, leading to a reduced BOLD in the rhythmic IAF flicker condition.

Sources that showed a near-zero difference in the evoked amplitude between rhythmic and arrhythmic IAF flicker could be explained by the model of superposition. In the BOLD domain, little change in the BOLD response to rhythmic IAF flicker as compared with arrhythmic IAF flicker at these sources would support an underlying mechanism of superposition: the intrinsic oscillatory activity, under both flicker conditions, would remain independent from the flicker, overlaid on which would be the evoked BOLD activity and given an equal number of flickers across both conditions, the BOLD response would be similar in both conditions. Thus, at sources identified in Experiment 2, we investigated the relationship between the evoked amplitude responses to rhythmic versus arrhythmic IAF flicker and the BOLD response to rhythmic versus arrhythmic IAF flicker.

5.5.1. Hypotheses. We hypothesised that there would be a significant predictive relationship of the BOLD signal difference between rhythmic and arrhythmic IAF flicker conditions on the evoked amplitude difference between rhythmic and arrhythmic IAF flicker conditions. Such a predictive relationship would corroborate the suggested underlying mechanisms to the evoked response patterns identified in Experiments 1 and 2.

6. Materials and methods

6.1. Experimental setup and design

6.1.1. Participants. Fifteen of the seventeen subjects described in Experiment 2 also participated in this fMRI study. One subject could not participate due to a metal implant and the other subject was excluded at the stage of EEG due to a lack of a discernible IAF peak (as described in section 2.3.2.).

6.1.2. Experimental setup. Ethical approval was given by the local ethics committee at the Technical University of Munich and informed consent was given by the participants. Subjects received financial remuneration for their participation. The experiment was conducted in a clinical 3T Philips Ingenia MR-Scanner (Philips Healthcare, Best, The Netherlands) using a 32-channel head coil, on top of which was a mirror (visual angle 70°) used for viewing the visual stimuli on a projector screen placed 1.5 metres behind the head of the participant. The nature of the visual stimulation was identical to that described in Experiments 1 and 2: a low-intensity checkerboard was projected onto the screen (In Focus LP530; projector-to-screen distance of 130cm) using Presentation software (Neurobehavioral Systems, http://www.neurobs.com). Placed directly in front of the projector was an LCD glass, the luminance of which was controlled by a microcontroller (Arduino Uno, Scarmagno, Italy), creating a flickering checkerboard stimulus at any flicker frequency of interest with a chosen duty cycle of 50%.

6.1.3. Experimental design. Subjects were simply instructed to focus on a central red fixation cross throughout the experiment and minimise any movement or blinking

artifact. Each subject completed two sessions of the visual stimulation, with each session consisting of fourteen flicker conditions: seven rhythmic flicker conditions, ranging from 7-12Hz in 1Hz steps plus the IAF, and seven arrhythmic conditions at the same frequencies. For a given frequency, arrhythmic stimulation was achieved by jittering the rhythmic cycle length by +/-25% and dividing this jittered cycle length by two to give a 50% duty cycle, for each flicker. As a result, average luminance, and number of flickers across each stimulation trial was kept constant across all conditions. Using a block design, each flicker condition was presented for 20 seconds, preceded always by a 50 second blank screen period to allow the BOLD signal to return to baseline. For this experiment, data across both sessions for the rhythmic IAF and arrhythmic IAF conditions only were analysed. This was to allow for comparison with the EEG data taken on the same day as described in Experiment 2. The goal was to relate the alpha oscillatory source responses to rhythmic versus arrhythmic IAF flicker in the EEG domain with that in the BOLD domain.

As Experiment 3 was conducted on the same day as Experiment 2, the IAF, as measured via EEG in Experiment 2 (see section 2.3.2.), was taken as the IAF for each subject in Experiment 3.

6.2. Imaging data acquisition

Whole-brain anatomical and functional images during visual stimulation were acquired for each participant. Anatomical images were acquired using a 3D magnetisation prepared rapid acquisition gradient echo sequence (TR = 7.4ms; TE = 3.3ms; inversion time TI = 656.7ms; flip angle = 8°; 227 sagittal slices; field of view = 240x240x170mm; matrix size = 320x320; reconstructed voxel size = 0.75mm^3).

Functional images consisting of 980 volumes were acquired using a single-shot echo-planar imaging sequence (EPI factor = 31; SENSE factor = 2; TR = 1000ms; TE = 30ms; flip angle = 70°; number of slices = 36 with a 0.2mm slice gap and transverse orientation; voxel size = $3mm^3$, field-of-view = 192x192x115mm; slice thickness = 3mm; matrix size = 64x62).

6.3. Imaging data analysis

6.3.1. Preprocessing. Preprocessing and analyses were conducted using SPM12 (Wellcome Department of Cognitive Neurology, London) as implicated in the DPARSF toolbox (v4.4. Advanced Edition, http://rfmri.org/DPARSF, Yan et al., 2016), using MATLAB (Mathworks, v2016b). Functional and anatomical images were manually reoriented to the AC/PC plane, following which the functional images across both sessions were realigned to the mean functional image using rigid body correction and head motion parameters were estimated. Four subjects showed excessive head motion (thresholded at 2mm translation/2° rotation in any direction) and hence were excluded from further analysis, leaving 11 subjects. The reoriented anatomical images were then coregistered and resliced to the mean functional image via rigid registration and segmented into probabilistic maps of gray matter (GM), white matter (WM) and cerebrospinal fluid (CSF) using the unified segmentation routine implemented in SPM. The maps were then entered into the DARTEL non-linear image registration procedure, which iteratively matches each template image to their own mean, increasing the image quality across iterations. Default settings as implemented in DPARSF were taken. The mean GM, WM, and CSF time series from the resulting probability maps thresholded at 99% were extracted and regressed from the realigned

functional images. Functional images were then normalised to MNI space with an isotropic voxel resolution of $3mm^3$, and smoothed with a $4mm^3$ FWHM Gaussian kernel, using the parameters generated by the DARTEL algorithm.

6.3.2. Data analysis: Predicted BOLD change to rhythmic vs. arrhythmic IAF flicker. For each of the remaining 11 subjects, the above steps left us with complete preprocessed fMRI datasets for each of the two sessions, spanning both rhythmic and arrhythmic visual stimulation periods and baselines. For each subject, these images were then entered in a first-level General Linear Model, with the six motion parameters entered as covariates of no interest. Each of the 28 stimulation conditions were modelled as box-car functions across the 20 seconds of stimulation, convolved with the canonical HRF and used as voxel wise regressors. Default parameters were taken for the model, apart from a masking threshold of 0.35, masked using a binarised (thresholded at 0.2), smoothed, normalised GM mask. The voxelwise beta images for each of the stimulation conditions were used for further analysis. Specifically, the four beta images corresponding to the rhythmic IAF and arrhythmic IAF stimulation for both sessions were analysed.

We were interested in the change in the BOLD signal (in terms of beta values) as a result of rhythmic IAF stimulation versus arrhythmic IAF stimulation. As reported in Part A, Experiment 2 revealed multiple sources of intrinsic alpha activity that showed variability in terms of their evoked responses to rhythmic versus arrhythmic IAF flicker, i.e., R-AR evoked amplitude. To probe the mechanistic underpinning of this variability, we investigated the difference in BOLD between rhythmic and arrhythmic IAF flicker stimulation at the same source locations as in Experiment 2, i.e., across 17 different

sources of occipitoparietal alpha oscillatory activity (concatenated across the 11 subjects included for analysis).

As described in section 2.4.1.,'Criterium 3', the likely source origin in MNI space of each of our 17 components was previously estimated. Using the MarsBaR software (v0.44, Brett et al. 2006, http://marsbar.sourceforge.net/index.html), For each subject, 10mm spherical regions-of-interest centred at the MNI coordinates of origin for each of the sources identified were created. The ROIs were overlaid on the beta images and the mean beta coefficients across all voxels per stimulation TR were extracted for the rhythmic and arrhythmic IAF conditions, for each session separately. For the rhythmic and arrhythmic IAF conditions, the mean beta coefficient across all 40 seconds of stimulation spanning both sessions was taken for each source, giving two mean beta values for each of the 17 sources for the rhythmic IAF condition and the arrhythmic IAF condition. Finally, the mean beta value for the arrhythmic IAF condition was subtracted from the mean beta value for the rhythmic IAF condition ('R-AR BOLD beta coefficient'), resulting in our BOLD outcome measure, per source, of the change in BOLD that occurs as a result of rhythmic IAF flicker relative to that of arrhythmic IAF flicker. A negative R-AR BOLD beta coefficient would indicate a reduced predicted BOLD change to rhythmic IAF flicker as compared with the change in BOLD to arrhythmic IAF flicker. A positive R-AR BOLD beta coefficient would indicate an increased predicted BOLD change to rhythmic IAF flicker as compared with the BOLD change to arrhythmic flicker. A near-zero R-AR BOLD beta coefficient would indicate little difference in the predicted BOLD change to rhythmic versus arrhythmic IAF flicker.

6.3.3. Statistical analysis. In order to take a closer look at the possible mechanistic underpinning of the source variability in evoked responses to the rhythmicity of IAF flicker as found in Experiment 2, the relationship between this BOLD difference beta value and the difference in evoked response to rhythmic and arrhythmic IAF flicker as identified in Experiment 2 (see section 2.5.2.) was investigated. One outlier was identified and removed at this stage so as to avoid violating the assumption of no outliers of further statistical tests, having an evoked response difference of 12.21, far outside the range of the other values (-1.3966:4.4991).

A linear mixed-effects model using the maximum-likelihood method was estimated to determine this relationship, with a fixed-effect predictor of the R-AR BOLD beta coefficients evoked responses, a random-effect factor of subject (with the intercept of the linear fitting varied across subjects to account for the violation of independence of data as a result of concatenation of multiple sources from any one subject) and the R-AR evoked amplitude values as the outcome variable. A p-value threshold of <.05 was used to determine statistical significance of the predictive model.

7. Results

As a means to investigate the potential mechanistic variability underlying the evoked response variability across alpha sources as discussed in Part A, the aim of Experiment 3 was to identify a predictive relationship of the R-AR BOLD beta coefficients on the R-AR evoked amplitude values (as described in Experiment 2), at sources of occipitoparietal alpha activity localised on the same day. The mean R-AR BOLD beta coefficient was -0.16583. A linear mixed-effect model analysis showed that there was no significant predictive value of the R-AR BOLD beta coefficients on the R-AR evoked amplitude values across sources ($F(1,14) = 1.946$; $p = 0.185$, $R^2 = 1.133$; standard error = 0.812; 95% CI [0.609 2.876]; see Figure 10).

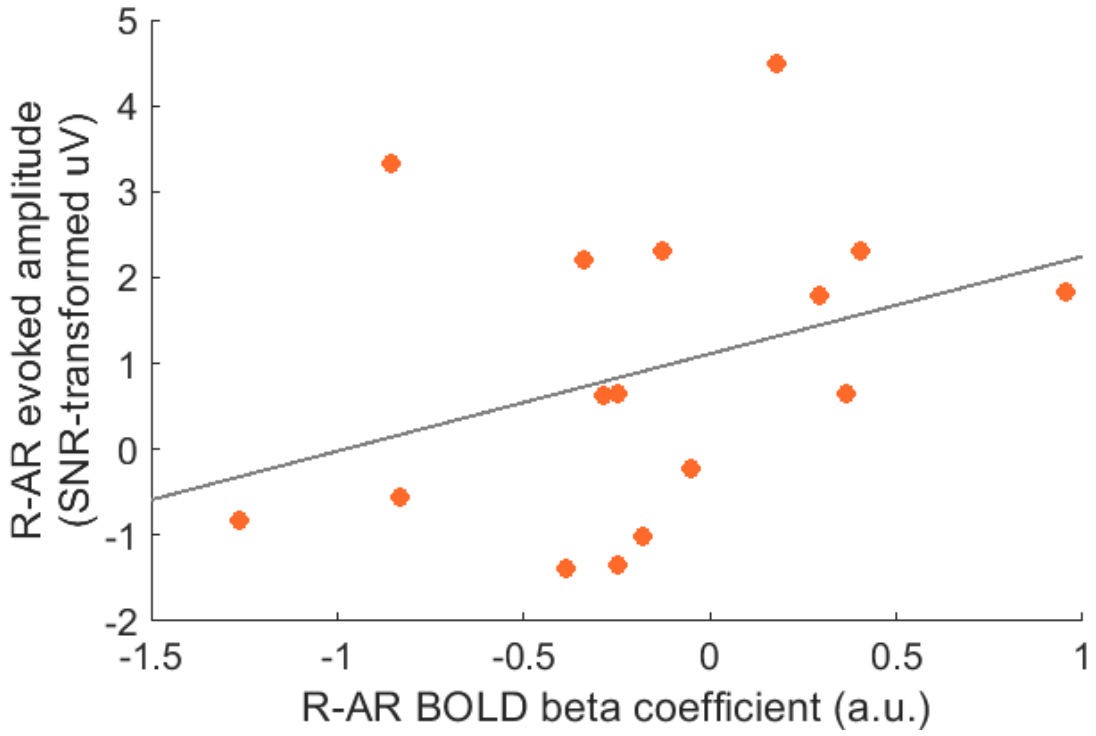

Figure 10. Scatterplot showing the relationship between the R-AR BOLD beta coefficients and the R-AR evoked amplitude values across sources of alpha oscillatory activity, with a least-squares best-fit line.

8. Discussion

8.1. No predictive relationship of the BOLD signal change on the evoked amplitude change to rhythmic vs. arrhythmic IAF flicker

The aim of Experiment 3 was to take advantage of the sensitivity of the BOLD signal to fluctuations in intrinsic alpha amplitude in order to infer the mechanistic underpinnings of the variability in evoked responses to visual flicker close to the IAF across sources of intrinsic alpha oscillatory activity as reported in Experiments 1 and 2.

In Experiments 1 and 2, we found some sources with evoked responses in line with a mechanism of entrainment. The mechanistic theory of entrainment postulates that the evoked response to rhythmic flicker is generated through the interaction with, and phase-alignment of, the intrinsic oscillator to the flicker. Since such an interaction with the intrinsic oscillator is not hypothesised to occur for arrhythmic flicker, increased evoked response amplitude at a given source generated via a mechanism of interaction with the intrinsic oscillator was hypothesised to be related to a reduced BOLD response to rhythmic versus arrhythmic IAF flicker.

In Experiments 1 and 2, we also found sources with evoked responses in line with a mechanism of superposition, whereby the flicker is assumed to remain independent from the intrinsic oscillator, with the evoked response linearly summated with the background oscillatory activity. In terms of the BOLD signal, we hypothesised we would see no change between rhythmic and arrhythmic IAF flicker: both conditions, given the same number of flickers across trials, would produce the same mean BOLD response.

To attribute such mechanistic underpinnings to the evoked responses observed in Experiments 1 and 2, we investigated the predictive relationship of the BOLD signal difference between rhythmic and arrhythmic IAF flicker on the evoked amplitude difference between the same conditions at sources identified in Experiment 2. If our evoked amplitude difference values (R-AR evoked amplitude values) could be attributed to different underlying mechanisms of entrainment and superposition, then we could expect to see a significant predictive relationship of the R-AR BOLD beta coefficients on the R-AR evoked amplitude values.

A significant predictive relationship between the two was not supported. The trend viewable in Figure 10 was in opposition to a trend we would have hypothesised: higher R-AR BOLD beta coefficients showed a trend towards higher R-AR evoked amplitude. The mean R-AR BOLD beta coefficient was a negative value, indicating that the majority of sources showed a reduced predicted BOLD change (beta coefficient) to rhythmic than arrhythmic IAF flicker. This finding was in line with the mean R-AR evoked amplitude difference being a positive value, indicating that the majority of sources showed an increased evoked amplitude to rhythmic versus arrhythmic IAF flicker. This suggests that, although a direct predictive relationship between the BOLD beta coefficients and the EEG evoked amplitude values was not supported, the anti-correlative relationship between the BOLD signal and intrinsic alpha amplitude was potentially still present.

8.2. Methodological issues, limitations, and strengths

The lack of a significant relationship could be attributed to a number of weaknesses in the study design.

8.2.1. Sample size. The low sample size, as in Experiments 1 and 2, is a definitive drawback of the study that could have meant that we simply did not have enough power to find a significant relationship. Sixteen data points (given the removal of the one outlier) across 11 subjects in a linear mixed model with one fixed and one random effects factor is potentially too low to identify a robust predictive relationship.

8.2.2. Temporal stability of sources. The sources were identified based on EEG data in Experiment 2, taken on the same day as Experiment 3. The non-stationary nature of EEG signals (Penny et al., 2002) makes it likely that the intrinsic alpha oscillatory sources identified in Experiment 2 were either no longer present at the same spatial location in Experiment 3 or showing different evoked response patterns to visual flicker. A simultaneous EEG-fMRI design would be the adequate design choice to overcome this problem of temporal uncertainty in source location and evoked responses.

8.2.3. Temporal stability of evoked responses. Our measures of evoked responses and BOLD responses to flicker were averaged across 20 seconds of data. Temporal variability even within this timeframe is inevitable in a dynamic non-stationary system and future analyses taking into account both the temporal and spatial variability would be more suited to the dynamic nature of the intrinsic alpha oscillatory system.

8.2.4. Changes in broadband power. Oscillatory activity is embedded on top of aperiodic broadband 1/f activity, which has shown to be physiologically relevant (He et al. 2010) and, importantly, temporally variant (Weber et al. 2020). The spectral slope has been attributed to changes in excitation and inhibition (Miller et al. 2009; Gao et al. 2017), whereas the offset has been related to the mean spiking activity of underlying

units (Manning et al. 2009). Not only was our BOLD measure susceptible to shifts in broadband power, which may have confounded our outcome measure, but also such shifts may hold relevant information related to changes in underlying oscillatory activity.

8.2.5. Subject arousal. Finally, the lack of a control of subject arousal is a confound of Experiment 3. The amplitude of evoked responses as well as the amplitude of intrinsic alpha activity has been shown to reflect arousal level (Näätänen & Picton, 1987; Coenen, 1998). Thus, misleading correlations between the two can occur based on subject vigilance. Future studies controlling for subject arousal would be advantageous.

8.3. Conclusion: No firm conclusions can be drawn as to the exact mechanistic underpinnings of the reported evoked response variability

The aim of Experiment 3 was to attribute mechanistic underpinnings to the evoked response variability reported in Experiments 1 and 2 by taking advantage of the sensitivity of the BOLD signal to intrinsic changes in alpha oscillatory activity. The non-simultaneous nature of the EEG and BOLD recordings is likely to have made a direct predictive relationship between the two unattainable due to the dynamic nature of oscillatory activity and hence we cannot draw any further conclusions as to which mechanisms underlie the evoked response variability reported in Experiments 1 and 2. A simultaneous EEG-fMRI design with a larger sample size, a design that allows for the spectral disentanglement of evoked from induced responses in the EEG domain and a control for subject arousal would be a much better suited design to identify the

variable mechanistic underpinnings of evoked responses at spatial sources to visual flicker.

Overall discussion and conclusion

The aim of this doctoral thesis was to investigate the presence of multiple underlying mechanisms of SSVEP generation across distinct sources of intrinsic alpha oscillatory activity. Two EEG experiments showed significant variability in the evoked responses to visual flicker stimulation across sources, suggesting the possibility of multiple underlying mechanisms. A third BOLD-fMRI experiment was conducted to identify changes in the intrinsic oscillators themselves, at the sources in Experiment 2, in order to draw clearer conclusions on the mechanistic underpinnings of evoked responses at the source level.

We did not identify a clear relationship between the evoked responses observed in Experiment 2 and the BOLD responses. Future studies may utilise a simultaneous EEG-fMRI design on a larger sample to accurately (in both spatial and also temporal terms) infer BOLD changes related to certain evoked responses to flicker. These experiments highlight the source level variability that is hidden at the traditional scalp level of EEG analysis and a dichotomous framework of SSVEP mechanism may be inaccurate; rather, our findings of significant variability suggest multiple mechanisms may exist across distinct sources of intrinsic alpha oscillatory activity.

References

Antonov, P. A., Chakravarthi, R., & Andersen, S. K. (2020). Too little, too late, and in the wrong place: Alpha band activity does not reflect an active mechanism of selective attention. *NeuroImage, 30*, 117006. https://doi.org/10.1016/j.neuroimage.2020.117006

Barzegaran, E., Vildavski, V. Y., & Knyazeva, M. G. (2017). Fine structure of posterior alpha rhythm in human EEG: Frequency components, their cortical sources, and temporal behavior. *Scientific Reports, 7*(1), 1–12.

Başar, E. (1980). EEG-brain dynamics: relation between EEG and brain evoked potentials. Elsevier-North-Holland Biomedical Press.

Becker, R., Reinacher, M., Freyer, F., Villringer, A., & Ritter, P. (2011, July 27). How ongoing neuronal oscillations account for evoked fMRI variability. *The Journal of Neuroscience: The Official Journal of the Society for Neuroscience, 31*(30), 11016–11027.

Benwell, C. S., London, R. E., Tagliabue, C. F., Veniero, D., Gross, J., Keitel, C., & Thut, G. (2019). Frequency and power of human alpha oscillations drift systematically with time-on-task. *NeuroImage, 192*, 101–114.

Berger, H. (1929). Über das elektroenkephalogramm des menschen. *Archiv für Psychiatrie und Nervenkrankheiten, 87*(1), 527–570.

Brandt, M. E., Jansen, B. H., & Carbonari, J. P. (1991). Pre-stimulus spectral EEG patterns and the visual evoked response. *Electroencephalography and Clinical Neurophysiology, 80*, 16–20.

Bressler, S. L. (1995, March 1). Large-scale cortical networks and cognition. *Brain Research. Brain Research Reviews, 20*(3), 288–304.

Buffalo, E. A., Fries, P., Landman, R., Buschman, T. J., & Desimone, R. (2011). Laminar differences in gamma and alpha coherence in the ventral stream. *Proceedings of the National Academy of Sciences of the United States of America, 108*(27), 11262–11267.

Busch, N. A., Dubois, J., & VanRullen, R. (2009). The phase of ongoing EEG oscillations predicts visual perception. *The Journal of Neuroscience: The Official Journal of the Society for Neuroscience, 29*(24), 7869–7876.

Buxton, R. B., Uludağ, K., Dubowitz, D. J., & Liu, T. T. (2004). Modeling the hemodynamic response to brain activation. *NeuroImage, 23*, S220–S233.

Buzsaki G. Rhythms of the Brain. Oxford University Press; 2006 Aug 3.

Capilla, A., Pazo-Alvarez, P., Darriba, A., Campo, P., & Gross, J. (2011). Steady-state visual evoked potentials can be explained by temporal superposition of transient event-related responses. *PLoS One, 6*(1), e14543.

Coenen, A. M. L. (1998). Neuronal phenomena associated with vigilance and consciousness: From cellular mechanisms to electroencephalographic patterns. *Consciousness and Cognition, 7*, 42–53.

Cohen, M. X. (2017). Rigor and replication in time-frequency analyses of cognitive electrophysiology data. *International Journal of Psychophysiology, 111*, 80–87. https://doi.org/10.1016/j.ijpsycho.2016.02.001

Cohen, M. X., & Gulbinaite, R. (2017). Rhythmic entrainment source separation: Optimizing analyses of neural responses to rhythmic sensory stimulation. *NeuroImage, 147*, 43–56.

Cole, S. R., & Voytek, B. (2017). Brain oscillations and the importance of waveform shape. *Trends in Cognitive Sciences, 21*(2), 137–149.

De Graaf, T. A., Gross, J., Paterson, G., Rusch, T., Sack, A. T., & Thut, G. (2013). Alpha-band rhythms in visual task performance: Phase-locking by rhythmic sensory stimulation. *PLoS One, 8*(3), e60035. https://doi.org/10.1371/journal.pone.0060035

Delorme, A., & Makeig, S. (2004). EEGLAB: An open source toolbox for analysis of single-trial EEG dynamics including independent component analysis. *Journal of Neuroscience Methods, 134*(1), 9–21.

Desikan, R. S., Ségonne, F., Fischl, B., Quinn, B. T., Dickerson, B. C., Blacker, D., . . . Albert, M. S. (2006). An automated labeling system for subdividing the human cerebral cortex on MRI scans into gyral based regions of interest. *NeuroImage, 31*(3), 968–980.

Di Russo, F., Pitzalis, S., Aprile, T., Spitoni, G., Patria, F., Stella, A., Spinelli, D., & Hillyard, S. A. (2007, April). Spatiotemporal analysis of the cortical sources of the steady-state visual evoked potential. *Human Brain Mapping, 28*(4), 323–334.

Dowsett, J., Dieterich, M., & Taylor, P. C. (2020). Mobile steady-state evoked potential recording: Dissociable neural effects of real-world navigation and visual stimulation. *Journal of Neuroscience Methods, 332*, 108540.

Engel, A. K., Fries, P., & Singer, W. (2001). Dynamic predictions: Oscillations and synchrony in top–down processing. *Nature Reviews. Neuroscience, 2*(10), 704–716.

Feige, B., Scheffler, K., Esposito, F., Di Salle, F., Hennig, J., & Seifritz, E. (2005). Cortical and subcortical correlates of electroencephalographic alpha rhythm modulation. *Journal of Neurophysiology, 93*(5), 2864–2872.

Fox, M. D., Snyder, A. Z., Zacks, J. M., & Raichle, M. E. (2006). Coherent spontaneous activity accounts for trial-to-trial variability in human evoked brain responses. *Nature Neuroscience, 9*(1), 23–25.

Fox, P. T., & Raichle, M. E. (1986). Focal physiological uncoupling of cerebral blood flow and oxidative metabolism during somatosensory stimulation in human subjects. *Proceedings of the National Academy of Sciences of the United States of America, 83*(4), 1140–1144.

Fries, P. (2005). A mechanism for cognitive dynamics: Neuronal communication through neuronal coherence. *Trends in Cognitive Sciences, 9*(10), 474–480.

Fries, P. (2009). Neuronal gamma-band synchronization as a fundamental process in cortical computation. *Annual Review of Neuroscience, 32*, 209–224.

Fuglø, D., Pedersen, H., Rostrup, E., Hansen, A. E., & Larsson, H. B. (2012). Correlation between single-trial visual evoked potentials and the blood oxygenation level dependent response in simultaneously recorded electroencephalography–functional magnetic resonance imaging. *Magnetic Resonance in Medicine, 68*(1), 252–260.

Gao, R., Peterson, E. J., & Voytek, B. (2017). Inferring synaptic excitation/inhibition balance from field potentials. *NeuroImage, 158*, 70–78.

Goldman, R. I., Stern, J. M., Engel, J., Jr., & Cohen, M. S. (2002). Simultaneous EEG and fMRI of the alpha rhythm. *Neuroreport, 13*(18), 2487.

Gray, M. J., Frey, H. P., Wilson, T. J., & Foxe, J. J. (2015). Oscillatory recruitment of bilateral visual cortex during spatial attention to competing rhythmic inputs. *The Journal of Neuroscience: The Official Journal of the Society for Neuroscience, 35*(14), 5489–5503.

Gulbinaite, R., van Viegen, T., Wieling, M., Cohen, M. X., & VanRullen, R. (2017). Individual alpha peak frequency predicts 10 Hz flicker effects on selective attention. *The Journal of Neuroscience: The Official Journal of the Society for Neuroscience, 37*(42), 10173–10184. https://doi.org/10.1523/JNEUROSCI.1163-17.2017

Haegens, S. (2020). Entrainment revisited: A commentary on Meyer, Sun, and Martin (2020). *Language, Cognition and Neuroscience, 1-5*. Advance online publication. https://doi.org/10.1080/23273798.2020.1758335

Haegens, S., Cousijn, H., Wallis, G., Harrison, P. J., & Nobre, A. C. (2014). Inter-and intra-individual variability in alpha peak frequency. *NeuroImage, 92*, 46–55.

Haller, M., Donoghue, T., Peterson, E., Varma, P., Sebastian, P., Gao, R., . . . Voytek, B. (2018). Parameterizing neural power spectra. BioRxiv, 299859 https://doi.org/10.1101/299859

Hanslmayr, S., Klimesch, W., Sauseng, P., Gruber, W., Doppelmayr, M., Freunberger, R., Pecherstorfer, T., & Birbaumer, N. (2007). Alpha phase reset contributes to the generation of ERPs. *Cerebral Cortex, 17*(1), 1–8.

He, B. J., Zempel, J. M., Snyder, A. Z., & Raichle, M. E. (2010). The temporal structures and functional significance of scale-free brain activity. *Neuron, 66*, 353–369. https://doi.org/10.1016/j.neuron.2010.04.020

Hermes, D., Nguyen, M., & Winawer, J. (2017). Neuronal synchrony and the relation between the blood-oxygen-level dependent response and the local field potential. *PLoS Biology, 15*(7), e2001461.

Herrmann, C. S. (2001). Human EEG responses to 1–100 Hz flicker: Resonance phenomena in visual cortex and their potential correlation to cognitive phenomena. *Experimental Brain Research, 137*(3-4), 346–353.

Hillyard, S. A., Hinrichs, H., Tempelmann, C., Morgan, S. T., Hansen, J. C., Scheich, H., & Heinze, H. J. (1997). Combining steady-state visual evoked potentials and fMRI to localize brain activity during selective attention. *Human Brain Mapping, 5*(4), 287–292.

Hughes, S. W., & Crunelli, V. (2005). Thalamic mechanisms of EEG alpha rhythms and their pathological implications. *The Neuroscientist, 11*(4), 357–372.

Jansen, B. H., Agarwal, G., Hegde, A., & Boutros, N. N. (2003). Phase synchronization of the ongoing EEG and auditory EP generation. *Clinical Neurophysiology, 114*(1), 79–85.

Jensen, O., & Mazaheri, A. (2010). Shaping functional architecture by oscillatory alpha activity: Gating by inhibition. *Frontiers in Human Neuroscience, 4*, 186.

Jensen, O., Gelfand, J., Kounios, J., & Lisman, J. E. (2002). Oscillations in the alpha band (9–12 Hz) increase with memory load during retention in a short-term memory task. *Cerebral Cortex (New York, N.Y.), 12*(8), 877–882.

Keitel, C., Keitel, A., Benwell, C. S., Daube, C., Thut, G., & Gross, J. (2019). Stimulus-driven brain rhythms within the alpha band: The attentional-modulation conundrum. *The Journal of Neuroscience: The Official Journal of the Society for Neuroscience, 39*(16), 3119–3129.

Keitel, C., Quigley, C., & Ruhnau, P. (2014). Stimulus-driven brain oscillations in the alpha range: Entrainment of intrinsic rhythms or frequency-following response? *The Journal of Neuroscience: The Official Journal of the Society for Neuroscience, 34*(31), 10137–10140.

Kirschstein, T., & Köhling, R. (2009). What is the source of the EEG? *Clinical EEG and Neuroscience, 40*(3), 146–149.

Koch, S. P., Steinbrink, J., Villringer, A., & Obrig, H. (2006). Synchronization between background activity and visually evoked potential is not mirrored by focal hyperoxygenation: Implications for the interpretation of vascular brain imaging. *The Journal of Neuroscience: The Official Journal of the Society for Neuroscience, 26*(18), 4940–4948.

Kwong, K. K., Belliveau, J. W., Chesler, D. A., Goldberg, I. E., Weisskoff, R. M., Poncelet, B. P., Kennedy, D. N., Hoppel, B. E., Cohen, M. S., & Turner, R. (1992). Dynamic magnetic resonance imaging of human brain activity during primary sensory stimulation. *Proceedings of the National Academy of Sciences of the United States of America, 89*(12), 5675–5679.

Laufs, H., Kleinschmidt, A., Beyerle, A., Eger, E., Salek-Haddadi, A., Preibisch, C., & Krakow, K. (2003). EEG-correlated fMRI of human alpha activity. *NeuroImage, 19*(4), 1463–1476.

Lauritzen, M. (2001). Relationship of spikes, synaptic activity, and local changes of cerebral blood flow. *Journal of Cerebral Blood Flow and Metabolism, 21*(12), 1367–1383.

Lauritzen, M., & Gold, L. (2003). Brain function and neurophysiological correlates of signals used in functional neuroimaging. *The Journal of Neuroscience: The Official Journal of the Society for Neuroscience, 23*(10), 3972–3980.

Lee, T. W., Girolami, M., & Sejnowski, T. J. (1999). Independent component analysis using an extended infomax algorithm for mixed subgaussian and supergaussian sources. *Neural Computation, 11*(2), 417–441.

Liu, Y., Bengson, J., Huang, H., Mangun, G. R., & Ding, M. (2016). Top-down modulation of neural activity in anticipatory visual attention: Control mechanisms revealed by simultaneous EEG-fMRI. *Cerebral Cortex, 26*(2), 517–529.

Liu, Y., Bengson, J., Huang, H., Mangun, G. R., & Ding, M. (2016). Top-down modulation of neural activity in anticipatory visual attention: Control mechanisms revealed by simultaneous EEG-fMRI. *Cerebral Cortex, 26*(2), 517–529.

Logothetis, N. K., Pauls, J., Augath, M., Trinath, T., & Oeltermann, A. (2001). Neurophysiological investigation of the basis of the fMRI signal. *Nature, 412*(6843), 150-157.

Logothetis, N. K. (2002). The neural basis of the blood–oxygen–level–dependent functional magnetic resonance imaging signal. *Philosophical Transactions of the Royal Society of London. Series B, Biological Sciences, 357*(1424), 1003–1037.

Logothetis, N. K. (2003). The underpinnings of the BOLD functional magnetic resonance imaging signal. *The Journal of Neuroscience: The Official Journal of the Society for Neuroscience, 23*(10), 3963–3971.

Logothetis, N. K. (2008). What we can do and what we cannot do with fMRI. *Nature, 453*(7197), 869–878.

Lopes da Silva, F. H., & Van Leeuwen, W. S. (1977). The cortical source of the alpha rhythm. *Neuroscience Letters, 6*(2-3), 237–241.

Lopes da Silva, F. H., Van Lierop, T. H., Schrijer, C. F., & Van Leeuwen, W. S. (1973). Organization of thalamic and cortical alpha rhythms: Spectra and coherences. *Electroencephalography and Clinical Neurophysiology, 35*(6), 627–639.

Lopes da Silva, F. H., Vos, J. E., Mooibroek, J., & Rotterdam, A. V. (1980). Relative contributions of intracortical and thalamo-cortical processes in the generation of alpha

rhythms, revealed by partial coherence analysis. *Electroencephalography and Clinical Neurophysiology, 50*, 449–456.

Lőrincz, M. L., Kékesi, K. A., Juhász, G., Crunelli, V., & Hughes, S. W. (2009). Temporal framing of thalamic relay-mode firing by phasic inhibition during the alpha rhythm. *Neuron, 63*(5), 683–696.

Makeig, S., Westerfield, M., Jung, T. P., Enghoff, S., Townsend, J., Courchesne, E., & Sejnowski, T. J. (2002). Dynamic brain sources of visual evoked responses. *Science, 295*(5555), 690–694.

Mäkinen, V., Tiitinen, H., & May, P. (2005). Auditory event-related responses are generated independently of ongoing brain activity. *NeuroImage, 24*(4), 961–968.

Manning, J. R., Jacobs, J., Fried, I., & Kahana, M. J. (2009). Broadband shifts in local field potential power spectra are correlated with single-neuron spiking in humans. *The Journal of Neuroscience: The Official Journal of the Society for Neuroscience, 29*, 13613–13620. https://doi.org/10.1523/JNEUROSCI.2041-09.2009

Mathewson, K. E., Prudhomme, C., Fabiani, M., Beck, D. M., Lleras, A., & Gratton, G. (2012). Making waves in the stream of consciousness: Entraining oscillations in EEG alpha and fluctuations in visual awareness with rhythmic visual stimulation. *Journal of Cognitive Neuroscience, 24*(12), 2321–2333.

Mayhew, S. D., & Bagshaw, A. P. (2017). Dynamic spatiotemporal variability of alpha-BOLD relationships during the resting-state and task-evoked responses. *NeuroImage, 155*, 120–137.

Mejias, J. F., Murray, J. D., Kennedy, H., & Wang, X. J. (2016). Feedforward and feedback frequency-dependent interactions in a large-scale laminar network of the primate cortex. *Science Advances, 2*(11), e1601335.

Miller, K. J., Sorensen, L. B., Ojemann, J. G., & den Nijs, M. (2009). Power-law scaling in the brain surface electric potential. *PLoS Computational Biology, 5*, e1000609.

Millet, D. (2002) The origins of EEG. In 7th Annual Meeting of the International Society for the History of the Neurosciences (ISHN).

Min, B. K., Busch, N. A., Debener, S., Kranczioch, C., Hanslmayr, S., & Engel, A. K. (2007). The best of both worlds: Phase-reset of human EEG alpha activity and additive power contribute to ERP generation. *International Journal of Psychophysiology, 65*(1), 58–68. https://doi.org/10.1016/j.ijpsycho.2007.03.002

Moosmann, M., Ritter, P., Krastel, I., Brink, A., Thees, S., Blankenburg, F., Taskin, B., Obrig, H., & Villringer, A. (2003). Correlates of alpha rhythm in functional magnetic resonance imaging and near infrared spectroscopy. *NeuroImage, 20*(1), 145–158.

Näätänen, R., & Picton, T. W. (1987). The N1 wave of the human electric and magnetic response to sound: A review and an analysis of the component structure. *Psychophysiology, 24*, 375–425.

Niedermeyer, E., & da Silva, F. L. (Eds.). (2005). Electroencephalography: basic principles, clinical applications, and related fields. Lippincott Williams & Wilkins.

Norcia, A. M., Appelbaum, L. G., Ales, J. M., Cottereau, B. R., & Rossion, B. (2015). The steady-state visual evoked potential in vision research: A review. *Journal of Vision (Charlottesville, Va.), 15*(6), 4.

Notbohm, A., & Herrmann, C. S. (2016). Flicker regularity is crucial for entrainment of alpha oscillations. *Frontiers in Human Neuroscience, 10*, 503.

Notbohm, A., Kurths, J., & Herrmann, C. S. (2016). Modification of brain oscillations via rhythmic light stimulation provides evidence for entrainment but not for superposition of event-related responses. *Frontiers in Human Neuroscience, 10*, 10. https://doi.org/10.3389/fnhum.2016.00010

Ogawa, S., Lee, T. M., Kay, A. R., & Tank, D. W. (1990). Brain magnetic resonance imaging with contrast dependent on blood oxygenation. *Proceedings of the National Academy of Sciences, 87*(24), 9868-9872.

Oostenveld, R., Fries, P., Maris, E., & Schoffelen, J. M. (2011). FieldTrip: Open source software for advanced analysis of MEG, EEG, and invasive electrophysiological data. *Computational Intelligence and Neuroscience, 2011*, 1–9. https://doi.org/10.1155/2011/156869

Ozus, B., Liu, H. L., Chen, L., Iyer, M. B., Fox, P. T., & Gao, J. H. (2001). Rate dependence of human visual cortical response due to brief stimulation: An event-related fMRI study. *Magnetic Resonance Imaging, 19*(1), 21–25.

Parkes, L. M., Fries, P., Kerskens, C. M., & Norris, D. G. (2004). Reduced BOLD response to periodic visual stimulation. *NeuroImage, 21*(1), 236–243.

Parkes, L. M., Fries, P., Kerskens, C. M., & Norris, D. G. (2004). Reduced BOLD response to periodic visual stimulation. *NeuroImage, 21*(1), 236–243.

Penny, W. D., Kiebel, S. J., Kilner, J. M., & Rugg, M. D. (2002). Event-related brain dynamics. *Trends in Neurosciences, 25*, 387–389.

Peterson, E. J., & Voytek, B. (2017). Alpha oscillations control cortical gain by modulating excitatory-inhibitory background activity. *Biorxiv*, 185074.

Pfurtscheller, G., Stancak, A., Jr., & Neuper, C. (1996). Event-related synchronization (ERS) in the alpha band—an electrophysiological correlate of cortical idling: A review. *International Journal of Psychophysiology, 24*(1-2), 39–46.

Pikovsky A, Kurths J, Rosenblum M, Kurths J. Synchronization: A Universal Concept in Nonlinear Sciences. Cambridge university press; 2003 Apr 24.

Rahn, E., & Başar, E. (1993a). Prestimulus EEG-activity strongly influences the auditory evoked vertex response: A new method for selective averaging. *The International Journal of Neuroscience, 69*, 207–220.

Rahn, E., & Başar, E. (1993b). Enhancement of visual evoked potentials by stimulation during low prestimulus EEG stages. *The International Journal of Neuroscience, 72*, 123–136.

Regan, D. (1989). Human brain electrophysiology. Evoked potentials and evoked magnetic fields in science and medicine. *The British Journal of Ophthalmology, 74*(4), 255.

Regan, D., & Heron, J. R. (1969). Clinical investigation of lesions of the visual pathway: A new objective technique. *Journal of Neurology, Neurosurgery, and Psychiatry, 32*(5), 479.

Saalmann, Y. B., Pinsk, M. A., Wang, L., Li, X., & Kastner, S. (2012). The pulvinar regulates information transmission between cortical areas based on attention demands. *Science, 337*(6095), 753–756.

Samaha, J., & Postle, B. R. (2015). The speed of alpha-band oscillations predicts the temporal resolution of visual perception. *Current Biology, 25*(22), 2985–2990.

Savers, B. M., Beagley, H. A., & Henshall, W. R. (1974). The mechanism of auditory evoked EEG responses. *Nature, 247*(5441), 481–483.

Scheeringa, R., Fries, P., Petersson, K. M., Oostenveld, R., Grothe, I., Norris, D. G., Hagoort, P., & Bastiaansen, M. C. (2011). Neuronal dynamics underlying high-and low-frequency EEG oscillations contribute independently to the human BOLD signal. *Neuron, 69*(3), 572–583.

Scheeringa, R., Petersson, K. M., Kleinschmidt, A., Jensen, O., & Bastiaansen, M. C. (2012). EEG alpha power modulation of fMRI resting-state connectivity. *Brain Connectivity, 2*(5), 254–264.

Scheeringa, R., Petersson, K. M., Oostenveld, R., Norris, D. G., Hagoort, P., & Bastiaansen, M. C. (2009). Trial-by-trial coupling between EEG and BOLD identifies networks related to alpha and theta EEG power increases during working memory maintenance. *NeuroImage, 44*(3), 1224–1238.

Schomer D. L., & Da Silva, F. L. (2012). Niedermeyer's Electroencephalography: Basic Principles, Clinical Applications, and Related Fields. Lippincott Williams & Wilkins; Oct 18.

Schürmann, M., Başar-Eroglu, C., & Başar, E. (1997). A possible role of evoked alpha in primary sensory processing: Common properties of cat intracranial recordings and human EEG and MEG. *International Journal of Psychophysiology, 26*(1-3), 149–170.

Schwab, K., Ligges, C., Jungmann, T., Hilgenfeld, B., Haueisen, J., & Witte, H. (2006). Alpha entrainment in human electroencephalogram and magnetoencephalogram recordings. *Neuroreport, 17*(17), 1829–1833.

Silva, L. R., Amitai, Y., & Connors, B. W. (1991). Intrinsic oscillations of neocortex generated by layer 5 pyramidal neurons. *Science, 251*(4992), 432–435.

Singer, W., & Gray, C. M. (1995). Visual feature integration and the temporal correlation hypothesis. *Annual Review of Neuroscience, 18*(1), 555–586.

Singh, M., Kim, S., & Kim, T. S. (2003). Correlation between BOLD-fMRI and EEG signal changes in response to visual stimulus frequency in humans. *Magnetic Resonance in Medicine: An Official Journal of the International Society for Magnetic Resonance in Medicine., 49*(1), 108–114.

Spaak, E., de Lange, F. P., & Jensen, O. (2014). Local entrainment of alpha oscillations by visual stimuli causes cyclic modulation of perception. *The Journal of Neuroscience: The Official Journal of the Society for Neuroscience, 34*(10), 3536–3544.

Spironelli, C., & Angrilli, A. (2017). Posture used in fMRI-PET elicits reduced cortical activity and altered hemispheric asymmetry with respect to sitting position: An EEG resting state study. *Frontiers in Human Neuroscience, 11*, 621.

Spironelli, C., Busenello, J., & Angrilli, A. (2016). Supine posture inhibits cortical activity: Evidence from Delta and Alpha EEG bands. *Neuropsychologia, 89*, 125–131.

Steriade, M., Gloor, P. L., Llinas, R. R., Da Silva, F. L., & Mesulam, M. M. (1990). Basic mechanisms of cerebral rhythmic activities. *Electroencephalography and Clinical Neurophysiology, 76*(6), 481–508.

Tass PA. Phase Resetting in Medicine and Biology: Stochastic Modelling and Data Analysis. Springer Science & Business Media; 2007 Jan 15.

Thibault, R. T., Lifshitz, M., Jones, J. M., & Raz, A. (2014). Posture alters human resting-state. *Cortex, 58*, 199–205.

Thut, G., Nietzel, A., Brandt, S. A., & Pascual-Leone, A. (2006). α-Band electroencephalographic activity over occipital cortex indexes visuospatial attention bias and predicts visual target detection. *The Journal of Neuroscience: The Official Journal of the Society for Neuroscience, 26*(37), 9494–9502.

Thut, G., Schyns, P., & Gross, J. (2011). Entrainment of perceptually relevant brain oscillations by non-invasive rhythmic stimulation of the human brain. *Frontiers in Psychology, 2*, 170.

Van Kerkoerle, T., Self, M. W., Dagnino, B., Gariel-Mathis, M. A., Poort, J., Van Der Togt, C., & Roelfsema, P. R. (2014). Alpha and gamma oscillations characterize

feedback and feedforward processing in monkey visual cortex. *Proceedings of the National Academy of Sciences, 111*(40), 14332-41.

Van Rossum, G., & Drake Jr., F. L. Python Reference Manual (v2.2.3). Centrum voor Wiskunde en Informatica Amsterdam: 2003 May 30.

Varela, F., Lachaux, J. P., Rodriguez, E., & Martinerie, J. (2001). The brainweb: phase synchronization and large-scale integration. *Nature Reviews Neuroscience, 2*(4), 229-39.

Wang, X. J. (2010). Neurophysiological and computational principles of cortical rhythms in cognition. *Physiological Reviews, 90*(3), 1195-268.

Weber, J., Klein, T., & Abeln, V. (2020). Shifts in broadband power and alpha peak frequency observed during long-term isolation. *Scientific Reports, 10*(1), 1-4.

Womelsdorf, T., Valiante, T. A., Sahin, N. T., Miller, K. J., & Tiesinga, P. (2014). Dynamic circuit motifs underlying rhythmic gain control, gating and integration. *Nature Neuroscience, 17*(8), 1031-9.

Yan, C. G., Wang, X. D., Zuo, X. N., & Zang, Y. F. (2016). DPABI: data processing & analysis for (resting-state) brain imaging. *Neuroinformatics, 14*(3), 339-51.

Acknowledgments

My first and foremost thanks go to my supervisor Dr. Christian Sorg and Dr. James Dowsett, for their unwavering guidance and support. I also thank the members of my PhD committee, Dr. Afra Wohlschläger and Prof. Dr. Markus Ploner, for their invaluable advice and fruitful discussions. I would also like to thank the Anaesthesiology department for their generosity and the administrative team of the MLST program. I would also like to thank my colleagues, not only for their help and advice, but also for gracing the last three academic years with joy and laughter.

Those who have supported me in the ways that I hold with the highest regard, are those that, ironically, probably don't believe they had much of an impact at all. But the reality is quite on the contrary. My wonderful Lukas, my family, and my friends, old and new. I sincerely thank you all.

It goes without saying that my acknowledgment of the support that I have received up to this point will be something that I will hold on to for the rest of my life. I consider myself extremely lucky to be surrounded by the most wonderful of people, without whom I would not have reached this milestone.

Scientific papers resulting from this PhD thesis

One original research article submitted to *NeuroImage*, currently under review.

Title

Evoked responses to rhythmic visual stimulation vary across sources of intrinsic alpha activity in humans

Author names and affiliations

Nuttall, R[1,2]; Jäger, C[1,2]; Zimmermann, J[1,2]; Archila Melendez, M. E[1,2]; Preibisch, C[1,2]; Taylor, P[3,4]; Sauseng, P[5]; Wohlschläger, A[1,2]; Sorg, C[1,2*]; Dowsett, J[1,2,4*]

[1]*Technical University of Munich, School of Medicine, TUM-Neuroimaging Center, Munich, Germany*

[2]*Technical University of Munich, School of Medicine, Department of Neuroradiology, Munich, Germany*

[3]*Ludwig Maximilian University, School of Medicine, Department of Neurology, Munich, Germany*

[4]*Ludwig Maximilian University, School of Medicine, German Center for Vertigo and Balance Disorders, Munich, Germany*

[5]*Ludwig Maximilian University, Munich Center for Neurosciences – Brain & Mind, Munich, Germany*

* both authors contributed equally